Sedimentary Geology 466 (2024) 106648

Contents lists available at ScienceDirect

Sedimentary Geology

journal homepage: www.elsevier.com/locate/sedgeo

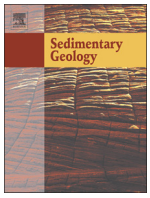

Linked evolution of Paleocene sea floor relief and deep marine currents in the Subbetic Zone, southern Spain

Victoriano Pujalte [a], Aitor Payros [a,*], Francisco J. Rodríguez-Tovar [b], Xabier Orue-Etxebarria [a], Naroa Martínez-Braceras [a]

[a] Department of Geology, Faculty of Science and Technology, University of the Basque Country (UPV/EHU), Ap. 644, E48080 Bilbao, Spain
[b] Department of Stratigraphy and Paleontology, Faculty of Science, University of Granada, 18002 Granada, Spain

ARTICLE INFO

Article history:
Received 1 February 2024
Received in revised form 11 April 2024
Accepted 12 April 2024
Available online 18 April 2024

Editor: Dr. Catherine Chagué

Keywords:
Microcodium
Deep sea sediments
Turbidites
Bottom-currents
Hemipelagites
Hiatuses

ABSTRACT

Paleocene deposits of the Subbetic Zone (southern Spain) provide outstanding evidence of the influence of sea mountains on deep marine currents. This part of the Betic Cordillera External Zones corresponds to the distal and deepest area of the original basin, where hemipelagic sedimentation prevailed during most of the Turonian-early Lutetian interval. This sedimentation is recorded by the so-called Capas Rojas and Quipar-Jorquera formations, units up to 250 m and 425 m thick, respectively, predominantly consisting of marls and marl/limestone alternations. These units draped and smoothed an irregular submarine topography of fault-bounded Mesozoic carbonate blocks. Some of these blocks became uplifted and subaerially exposed after a mid-Danian tectonic episode, transforming the Subbetic Zone in an archipelago during the late Danian-early Selandian interval. The emerged blocks were colonized by *Microcodium*-producing terrestrial plants, *Microcodium* consisting of aggregates of submilimetric monocrystalline calcite grains. Massive resedimentation of these grains into depressed zones of the archipelago resulted in discrete accumulations up to 100 m thick but of comparatively modest extent (≤150 km^2) of calcarenites rich in *Microcodium* remains. The study of one of these calcarenite units, the Olivares Formation, demonstrates that most of its constituent *Microcodium* remains were brought to the deep sea by turbidity currents, but were subsequently reworked by oscillatory and unidirectional bottom-currents. The analysis of the Capas Rojas Formation in its type section and surrounding areas, where *Microcodium*-rich calcarenites are absent, demonstrates that the Danian-Selandian succession is riddled with hiatuses, which resulted in a drastic thickness reduction of the interval. Clearly, the rugged sea floor topography resulting from the mid-Danian tectonic event enhanced the sedimentary transport capacity of bottom-currents that, in addition to piling-up *Microcodium*-rich calcarenites in restricted zones, disturbed the hemipelagic sedimentation elsewhere in the Subbetic Zone. From late Thanetian times onwards the background hemipelagic sedimentation typical of the Capas Rojas progressively resumed throughout the Subbetic Zone, recording the gradual abatement of the sea floor relief by protracted erosion and/or subsidence.

1. Introduction

The existence of two main groups of deep sea sediments, (hemi)pelagic and clastic, has long been recognized. The former, which usually accumulate slowly by gravity settling, consist of mixtures in variable proportions of calcareous or siliceous shells of microorganisms (foraminifera, calcareous nannoplankton, radiolaria, etc.), clays and fine silt-size inorganic particles (Hüneke and Henrich, 2011).

Clastic deposits, either siliciclastic, calciclastic, or mixtures of both types, are medium silt to boulder sized and much more varied. These sediments are mainly delivered to the deep sea by mass-failures (e.g., slumps, debris-flows) and turbidity currents. Some of these sediments can be later reworked by contour currents and re-deposited as contourites. However, as aptly pointed out by Rebesco et al. (2017; their Fig. 1), pure mass-transport accumulations, turbidites and contourites must be regarded as the end-members of a whole range of "hybrid" deep sea clastics, since each of the three processes may evolve from one to another and deposits of one process may be reworked by a different one. For instance, Barnolas and Teixell (1994) and Payros et al. (1999) documented the transformation of Eocene disorganized megabreccias resulting from vast collapses of carbonate platform margin into turbidites, while the coexistence and/or interactions of turbidites and contourites have been reported by several authors (e.g., Ito,

* Corresponding author.
E-mail address: a.payros@ehu.eus (A. Payros).

https://doi.org/10.1016/j.sedgeo.2024.106648

2002; Brackenridge et al., 2013; Alonso et al., 2016; Rodríguez-Tovar and Hernández-Molina, 2018; Rodríguez-Tovar et al., 2019, 2022; de Castro et al., 2020; Hüneke et al., 2021; Miguez-Salas and Rodríguez-Tovar, 2021; Hernández-Molina et al., 2022a, 2022b). Besides, it is becoming increasingly clear that, in addition to contour currents, deep sea sediments can also be reworked by other processes, notably by oceanic deep waves, of which recent investigations have demonstrated both their ubiquity (e.g., Jackson, 2004; Santo et al., 2005; St. Laurent et al., 2012; Huang et al., 2023), and their imprint on ancient sediments (e.g., Pomar et al., 2012, and references therein). More recently turbulent upslope currents along the flanks of submarine mountains have also been documented (Voosen, 2022). Therefore, the range of "hybrid" deep sea deposits is likely to be greater than hitherto realized.

The late Cretaceous-Ypresian interval is represented in the Subbetic Zone of southern Spain by two distinct types of sedimentary accumulations. The most extensive of them, included in the correlative Capas Rojas and Quipar-Jorquera formations, primarily consists of marls rich in planktonic foraminifera and calcareous nannoplankton. These marls are commonly interpreted as slowly accumulated hemipelagites (Vera and Molina, 1999; Vera, 2000). The other one is mainly composed of a peculiar type of calcarenites that comprise up to 90 % of *Microcodium* remains. Their peculiarity lies in the fact that *Microcodium* is widely accepted to originate in subaerial carbonate rich substrates and soils, either within roots of terrestrial plants (e.g., Klappa, 1978; Smit, 1979; Alonso-Zarza et al., 1998; Košir, 2004, 2015), or else as a result of actinobacterial activity (Kabanov et al., 2008). The most common variety of authochtonous *Microcodium* consists of aggregates of monocrystalline grains of calcite 0.1–1 mm long arranged radially around a central axis ("corn-cob" arrangement). These grains are highly resistant and can endure resedimentation into shallow and deep marine settings (e.g., Smit, 1979; Martín-Algarra, 1987; Molina et al., 2006; Pujalte et al., 2019). Units of calcarenites rich in resedimented *Microcodium* remains are dispersed throughout the Subbetic Zone, consistently intercalated within hemipelagic marls (Fig. 1A, B). It is presumed that these units either adjoin faults or gradually thin out laterally, as there has been no observation of intermingling between the calcarenites and hemipelagic marls. They can exceed 100 m in thickness but typically have relatively limited lateral extent, covering areas of 50–150 km^2. They have either

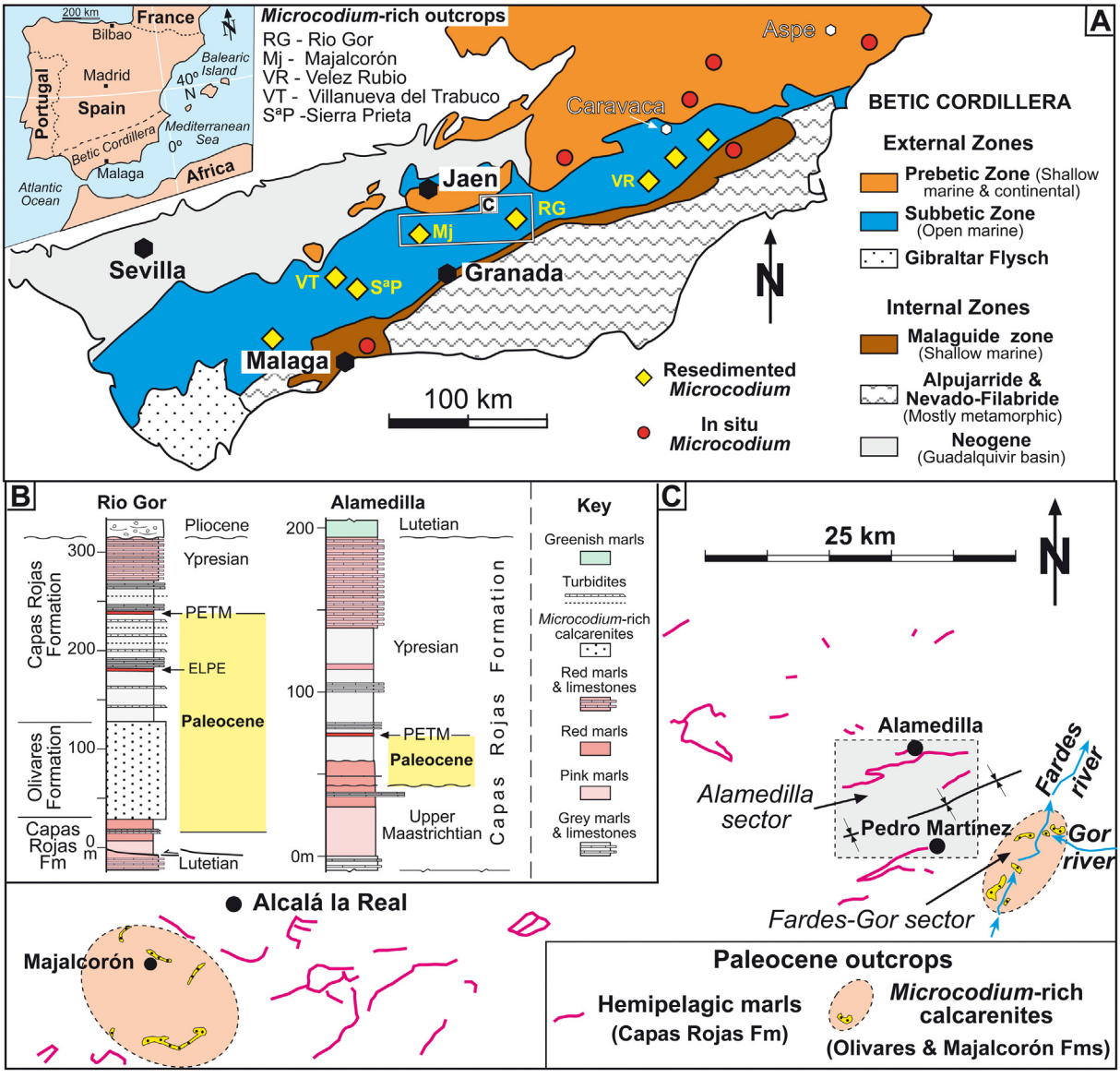

Fig. 1. (A) Simplified geological map of the Betic Cordillera with indication of the occurrences of in situ and resedimented *Microcodium* (based on data of Smit, 1979; Martín-Algarra, 1987; Molina et al., 2006, and our own observations), with localities and outcrops mentioned in the text. The present day situation of the Cordillera is shown in the inset, the white lines indicating the 0° meridian (Greenwich) and the 40° N parallel. (B) Simplified lithological columns of the Rio Gor and Alamedilla reference sections. (C) Outcrop map of the two types of upper Maastrichtian-Paleocene deposits recognized in the central part of the Subbetic Zone, with location of the Fardes-Gor and Alamedilla sectors.

been interpreted as turbidites (e.g., Comas, 1978; Smit, 1979) or as shallow marine tempestites (Vera et al., 2004; Molina et al., 2006). One purpose of this paper is to re-asses these interpretations, with new data, in the light of recent advances in the knowledge of deep sea sedimentary processes. A second purpose is to discuss the influence that submarine palaeotopography exerted on these processes.

2. Geological setting

This study focuses on two sectors of the central part of the Subbetic Zone of southeastern Spain, Alamedilla and Fardes-Rio Gor (Fig. 1). Additionally, it incorporates information from the western and eastern parts of this Zone gleaned from the geological literature. The Subbetic Zone, which is the distal part of the Betic Cordillera External Zones, (Fig. 1A), is located seawards of the shallow marine Prebetic Zone and contains a thick Triassic to lower Miocene sedimentary succession accumulated mostly in open marine conditions, on the southern margin of the Iberian Plate and, thus, on the north-westernmost part of the Tethys Ocean. The Betic External Zones were tectonically deformed during Miocene times by an oblique transcurrent collision with the allochthonous Betic Internal Zones (Fig. 1A; Vera, 2004; Martínez del Olmo, 2018; Sanz de Galdeano, 2019).

The late Maastrichtian-early Ypresian interval is represented in the study area, as in the rest of the Subbetic Zone, by two very different types of successions (Fig. 1B, C). The most extensive of them mainly comprises accumulations of hemipelagic marls rich in planktonic

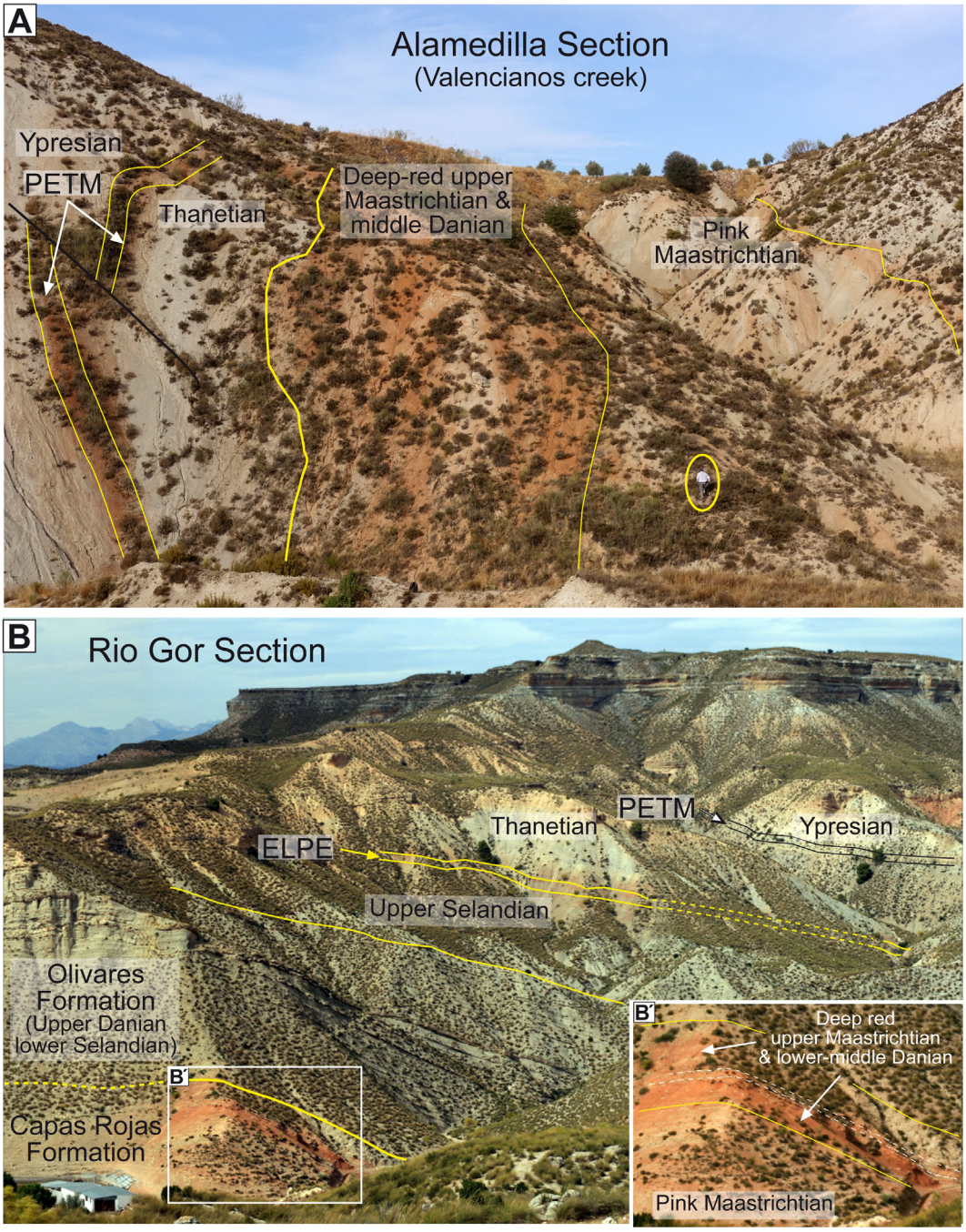

Fig. 2. Field views of representative sections containing the two types of Maastrichtian-Paleocene successions recognized in the central part of the Subbetic Zone: (A) Alamedilla section (encircled geologist for scale). (B) Rio Gor; (B′) enlarged view of part of the Capas Rojas Formation underlying the Olivares Formation (ELPE: Early-Late Paleocene Event; PETM: Paleocene-Eocene Thermal Maximum); the white broken lines in B′ indicate two prominent calcarenite beds. Explanation within the text.

microfossils (e.g., Martínez-Gallego, 1977; El Mamoune, 1996), which locally intercalate lesser proportions of calciturbidites. These marls belong to the Capas Rojas Formation, a widespread unit spanning the late Cretaceous–early Eocene interval (Vera and Molina, 1999). Successions of the second type are chronostratigraphically restricted to the late Danian-early Selandian interval and have a very different character, as they are largely made up of *Microcodium*-rich calcarenites.

Alamedilla and Río Gor are two representative sections comprising both types of accumulations. At Alamedilla, which is the type section of the Capas Rojas Formation (Vera et al., 1982), the Paleocene succession is just about 30 m thick and consists almost exclusively of hemipelagic marls, of which 14 m belong to the Danian and the remaining 16 m to the Thanetian, the Selandian being absent (Figs. 1B, 2A). In the Rio Gor section the Paleocene is 267 m thick and seems to be biostratigraphically complete (Pujalte et al., 2017; Figs. 1B, 2B). In this section the late Danian-early Selandian interval is represented by a *Microcodium*-rich calcarenite unit defined as Olivares Formation (Comas, 1978), which concordantly overlies the Capas Rojas Formation (Figs. 1B, 2B). The Olivares Formation is concordantly overlain by a ca. 120 m thick upper Selandian-lower Ypresian succession mainly composed of gray marls with minor intercalations of hemipelagic limestones and bioclastic turbidites (Pujalte et al., 2017). This succession, which also belongs to the Capas Rojas Formation, includes the record of two important hyperthermal events: the Early-Late Paleocene Event (ELPE) and the Paleocene-Eocene Thermal Event (PETM) (Fig. 2B). The former hyperthermal is known to occur just below the Selandian/Thanetian boundary (Bernaola et al., 2007; Schmitz et al., 2011; Pujalte et al., 2014a), while the base of the latter marks the Paleocene/Eocene boundary (Aubry et al., 2007; Pujalte et al., 2019).

A unit of the same age and composition as the Olivares Formation, situated to the south of the Alcala la Real village (Fig. 1C), was formally defined as Majalcoron Formation by Vera et al. (2004). The rest of the *Microcodium*-rich units scattered throughout the Subbetic Zone have a similar age (Fig. 1A). Their massive content in *Microcodium* remains requires the existence of nearby emergent calcareous reliefs (Martín-

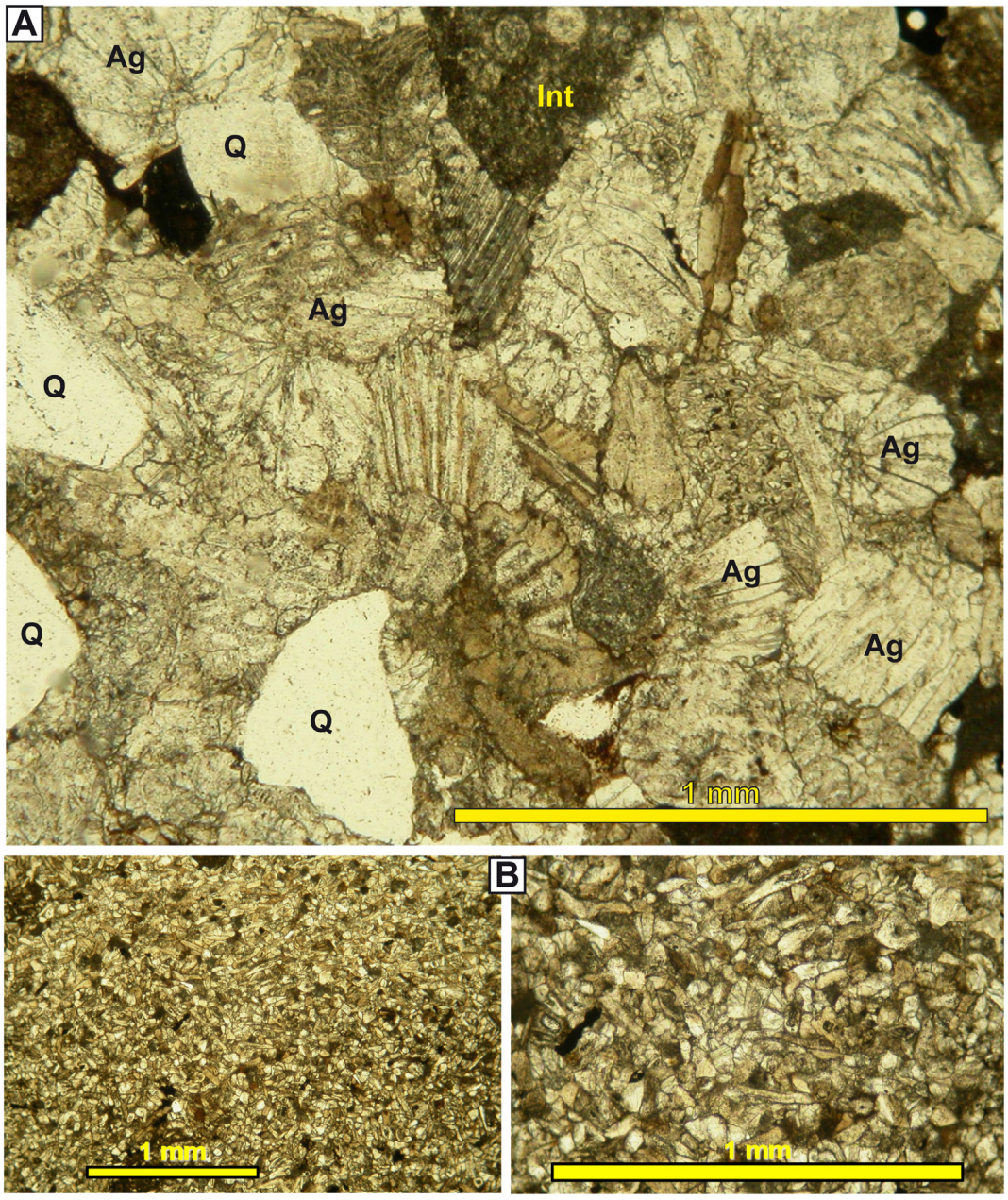

Fig. 3. Thin section micrographs illustrating the most representative microfacies of the Olivares Formation. (A) From medium/thick-bedded calcarenites showing: *Microcodium* aggregates (Ag); Quartz (Q); Intraclasts (Int), one with calpionellids. (B) From thin/very thin-bedded calcarenites almost exclusively composed of *Microcodium* grains.

Algarra, 1987; Pujalte et al., 2019; Rodriguez-Tovar et al., 2020), which entails that the paleogeography of the Subbetic Zone during the late Danian-early Selandian was akin to an archipelago.

3. Methods and data set

The study area comprises two sectors of the Subbetic Zone that contain the stratotypes of the Olivares and the Capas Rojas Formations, the former situated around the confluence of the Fardes and Gor river valleys, the latter in the outskirts of the village of Alamedilla (Fig. 1C). Methods include mapping, logging/sampling of six reference sections, analyses of sedimentary facies and palaeocurrents in the field, and of microfacies and micropalaeontology in the laboratory. The microfacies were analyzed in 91 thin-sections at the Department of Stratigraphy and Paleontology of the University of Granada with an Olimpus microscope with an attached AxioCam MRC Zeiss, with which micrographs of representative microfacies were obtained (Fig. 3). Dating was attained through the study with a binocular microscope of planktonic

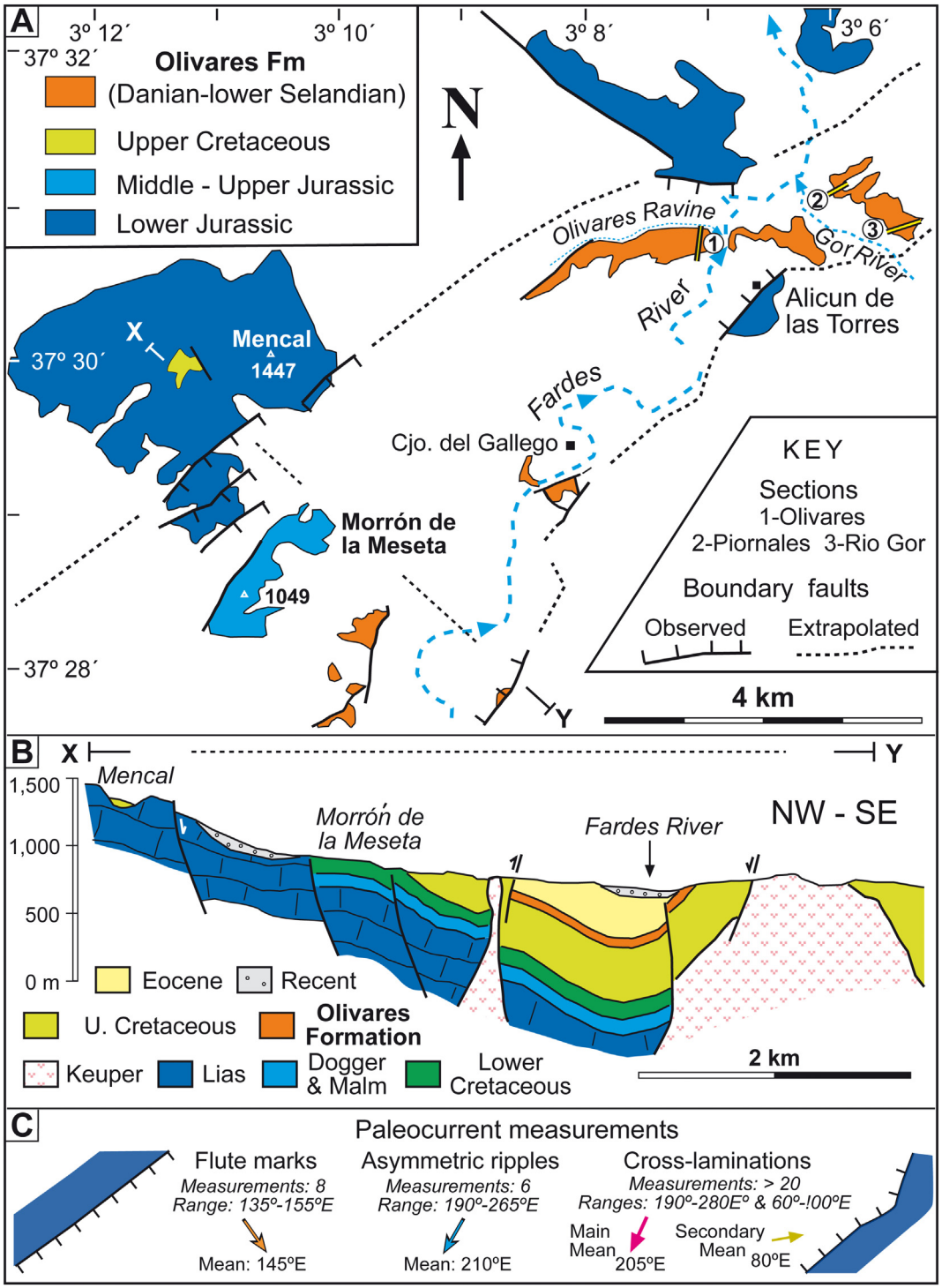

Fig. 4. (A) Outcrop map of the Olivares Formation in the Fardes and Gor river valleys, with location of the three sections discussed in this paper; note the fault-bounded Jurassic Massifs surrounding the valleys. (B) Structural cross-section across transect X-Y (location in A; modified from Comas et al., 1973). (C) Summary of palaeocurrent measurements from different directional structures and bedforms of the Olivares Formation.

foraminifera washed from marly samples at the Department of Geology of the University of the Basque Country. For this task, data reported by Pujalte et al. (2012, 2014b) was complemented with new samples collected for this study. All in all, 75 marly samples from both sectors were analyzed. In addition, the planktonic foraminifera information of Martínez-Gallego (1977), who sampled at high resolution three sections of the Alamedilla sector, has been re-evaluated applying the zonation criteria of Wade et al. (2011; Fig. S1).

The Olivares Formation was inspected in three sections (Olivares, Piornales and Rio Gor, Figs. 4A, S2). The thickness of its constituent calcarenite beds varies widely, the terminology of Tucker (1982) having been adopted for their description: very thin, 1–3 cm; thin, 3–10 cm; medium, 10–30 cm; thick, 30–100 cm; very thick >100 cm. Palaeocurrents were measured from flute marks, parting lineations, ripples and cross laminations.

The Alamedilla sector is located in the north flank of a wide, low relief synclinorium (Fig. 1C). For this study the late Maastrichtian-early Eocene interval of the Capas Rojas Formation was revisited, with emphasis on the Paleocene interval. The best exposed part of the sector was mapped with the help of color satellite images of Google Earth and four sections were logged in detail.

4. Results

4.1. The Capas Rojas Formation in the Fardes-Gor sector

In the Rio Gor section, the best outcrop of Fardes-Gor sector, the 67 m thick part of the Capas Rojas Formation underlying the Olivares Formation is composed of marls interspersed with occasional thin-bedded calciturbidites rich in tests of planktonic foraminifera. The

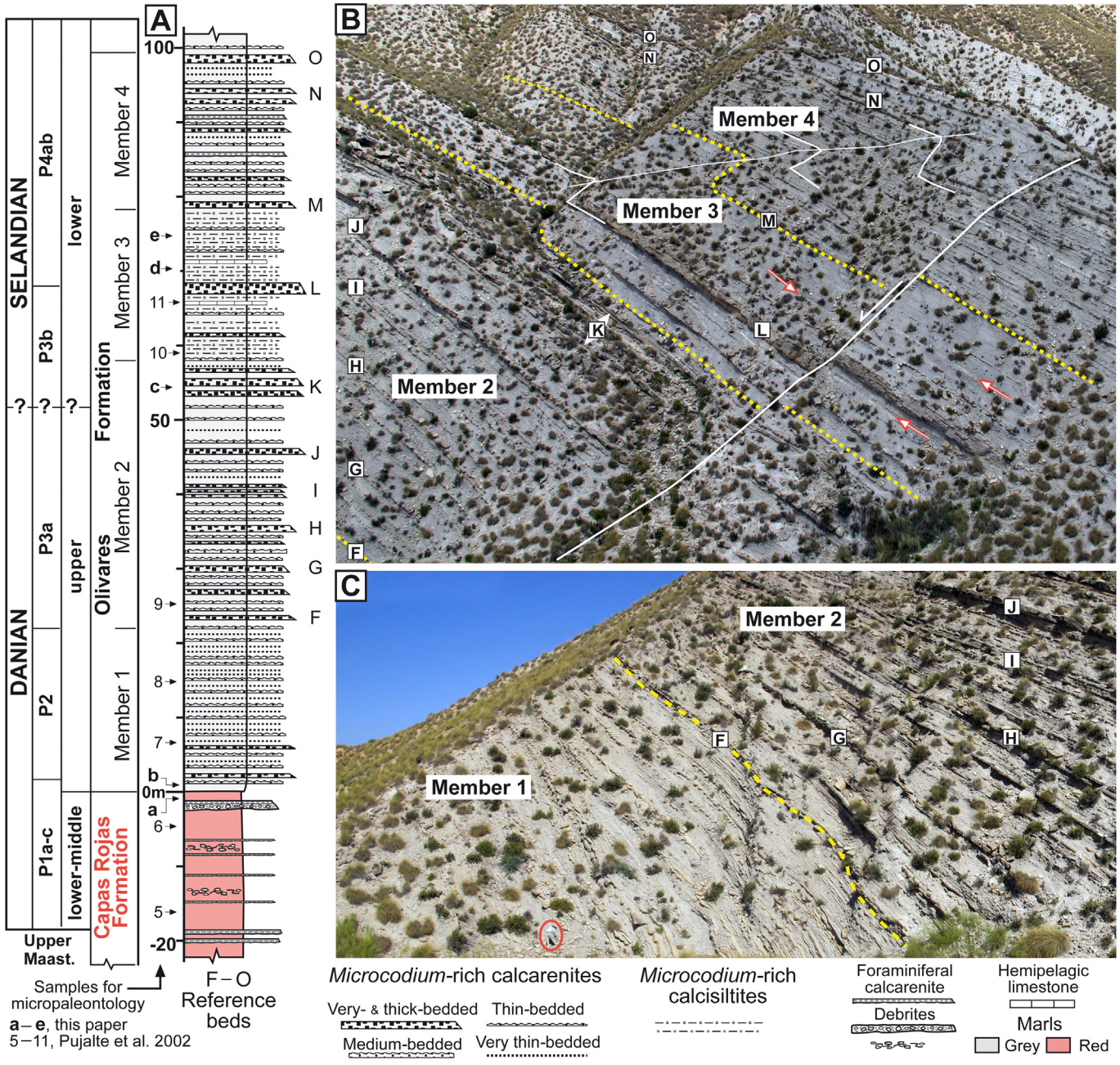

Fig. 5. (A) Lithostratigraphic column of the upper Maastrichtian-lower Selandian segment of the Rio Gor section with indication of planktonic foraminifera zonation, sample location and reference medium- and thick-bedded calcarenites of the Olivares Formation. (B, C) Field views of the Olivares Formation (encircled geologist in C gives scale; reference calcarenite beds F–J, visible in both images, help to connect them). The red arrows in B indicate limestone beds with planktonic foraminifera from Member 3.

marls of the lower 40 m of the section exhibit pink hues, while those of the upper 27 m have deep red tones and intercalate two prominent turbidites, each about 50 cm thick (Fig. 2B, B′). The pink marls and the part of the deep red marls underlying the upper prominent turbidite contain *Abathompalus mayaroensis*, the index planktonic foraminifera species of the latest Maastrichtian biozone. Instead, the deep red marls above the upper prominent turbidite pertain to the early Danian planktonic foraminifera biozone P1 of Wade et al. (2011). Consequently, the deep red marls encompass the Cretaceous-Palaeogene transition, though the precise location of the K/Pg boundary itself remains elusive, potentially obscured by a minor hiatus.

About 1 m below the top of the Capas Rojas Formation there exists a conspicuous mass-wasting accumulation, also recognized with different characteristics in the other two sections studied in the Fardes-Gor sector. In the Olivares section it is represented by a chaotic debris flow deposit >4 m thick (base not outcropped), which includes a limestone clast, 1.4 × 2.8 m across, set within a matrix of smaller marl and limestone clasts (Fig. S3A). In the other two sections the accumulation consists of a graded debrite/turbidite couplet 2.10 m thick at Piornales and 1.80 m thick at Rio Gor (Fig. S3B). The outsized limestone clast at Olivares contains planktonic foraminifera, probably globotruncanids, rugoglobigerinids and hedbergellids, a late Cretaceous association (Fig. S3C). Some clasts of the graded debrite at Rio Gor are solely composed of densely stacked thin-shelled bivalves, probably of the genus *Bositra* (Fig. S3D). Autochthonous accumulations with this facies have been described in mid-Jurassic carbonates of the Subbetic Zone (e.g. Molina et al., 2007). The overlying turbidite contains fragments of bivalves, echinoderms, possible coralline algae, bryozoans, a few *Microcodium* aggregates and, notably, thick-shelled benthic foraminifera (Fig. S3E, F). This association, especially the benthic foraminifera, suggests that the top part of the Massifs bordering the graben were in shallow marine conditions, the sporadic presence of *Microcodium* aggregates implying that certain portions may have already been above water.

4.2. Olivares Formation

4.2.1. Setting and general features

The Olivares Formation of the Fardes-Gor sector is a key unit for the purposes of this paper. Therefore, the results from this unit are described far more extensively than those from the Capas Rojas Formation. Outcrops of the Olivares Formation are restricted to a comparatively narrow graben bounded by faulted blocks of Jurassic and Cretaceous carbonate rocks, some of them partly buried by upper Eocene and younger deposits (Fig. 4A, B). The unit is about 65 m thick in the Olivares section, its thickness increasing eastward gradually to up to 100 m in the Rio Gor section. Palaeocurrents from occasional flute marks (8 measurements) consistently indicate south-eastwards transport

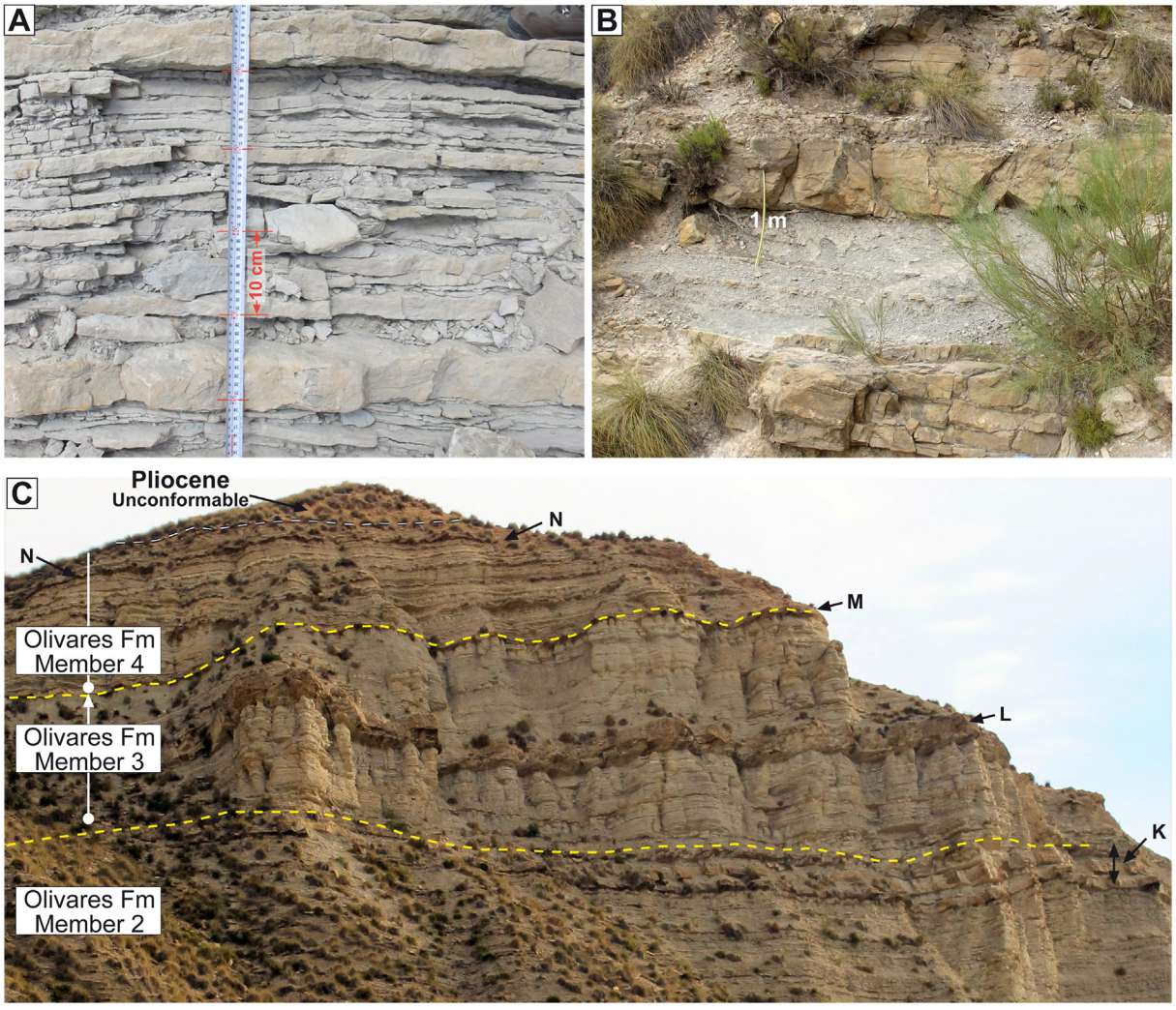

Fig. 6. Field images illustrating representative lithofacies of the four members of the Olivares Formation in the Rio Gor section: (A) Member 1, prevalence of very thin- and thin-bedded *Microcodium*-rich calcarenites. (B) Member 2, medium- and thick-bedded *Microcodium*-rich calcarenites intercalated within very thin- and thin-bedded calcarenites. (C) General view of Members 3 and 4 in a cliff just west of the section (for location see Fig. 7C). Description of both members within the text.

(mean direction toward 145°E, Fig. 4C), away from the Mesozoic blocks of the NW margin of the graben, which likely were the source of most, if not all, the *Microcodium* remains (Pujalte et al., 2019). A few examples of parting lineation have been observed, their orientation being as a rule parallel to the flutes (Fig. S4A, B). Instead, palaeocurrents from asymmetrical ripples preserved on top surfaces of strata (Fig. S4C, D) are more variable, their mean value (210°E) being near parallel to the elongation of the graben (Fig. 4C). Internal cross-laminations are ubiquitous but, with few exceptions, are only visible in two-dimension exposures (see below), from which fully reliable palaeocurrents cannot be obtained. Measurements of >20 of these cross-laminations (biased by the orientation of the exposures) can be separated in two groups, the main one with a range between 190° and 280°E (mean toward 205°E), the secondary one with a range between 60° and 100°E (mean toward 80°E) (Fig. 4C). A few examples of symmetrical ripples have also been observed (Fig. S4E, F).

4.2.2. Stratigraphy

The stratigraphy of the Olivares Formation presented herein is a refined version of prior schemes by Pujalte et al. (2017) and by Rodriguez-Tovar et al. (2020), based on the new data acquired in this study. It was established at the Rio Gor section, which is the most complete and accessible of the unit in the study area (Figs. 2, S2C).

In the Rio Gor section the bulk of the Olivares Formation consists of *Microcodium*-rich light-gray calcarenites and calcisiltites, with lesser proportions of bioclastic calcarenites, calcarenites of mixed composition (planktonic foraminifera tests and *Microcodium* remains), marls and a few beds of hemipelagic limestones (Fig. 5). These deposits are usually stratified in plane-parallel beds ranging in thickness from 1 cm to 1.65 m (Figs. 5, 6). The relative proportions of these lithologies vary upsection and, accordingly, four successive Members, coded 1–4, have been distinguished (Fig. 5), which are also recognizable in the other two studied sections of the unit (Fig. S2). Members 1 and 2 correspond,

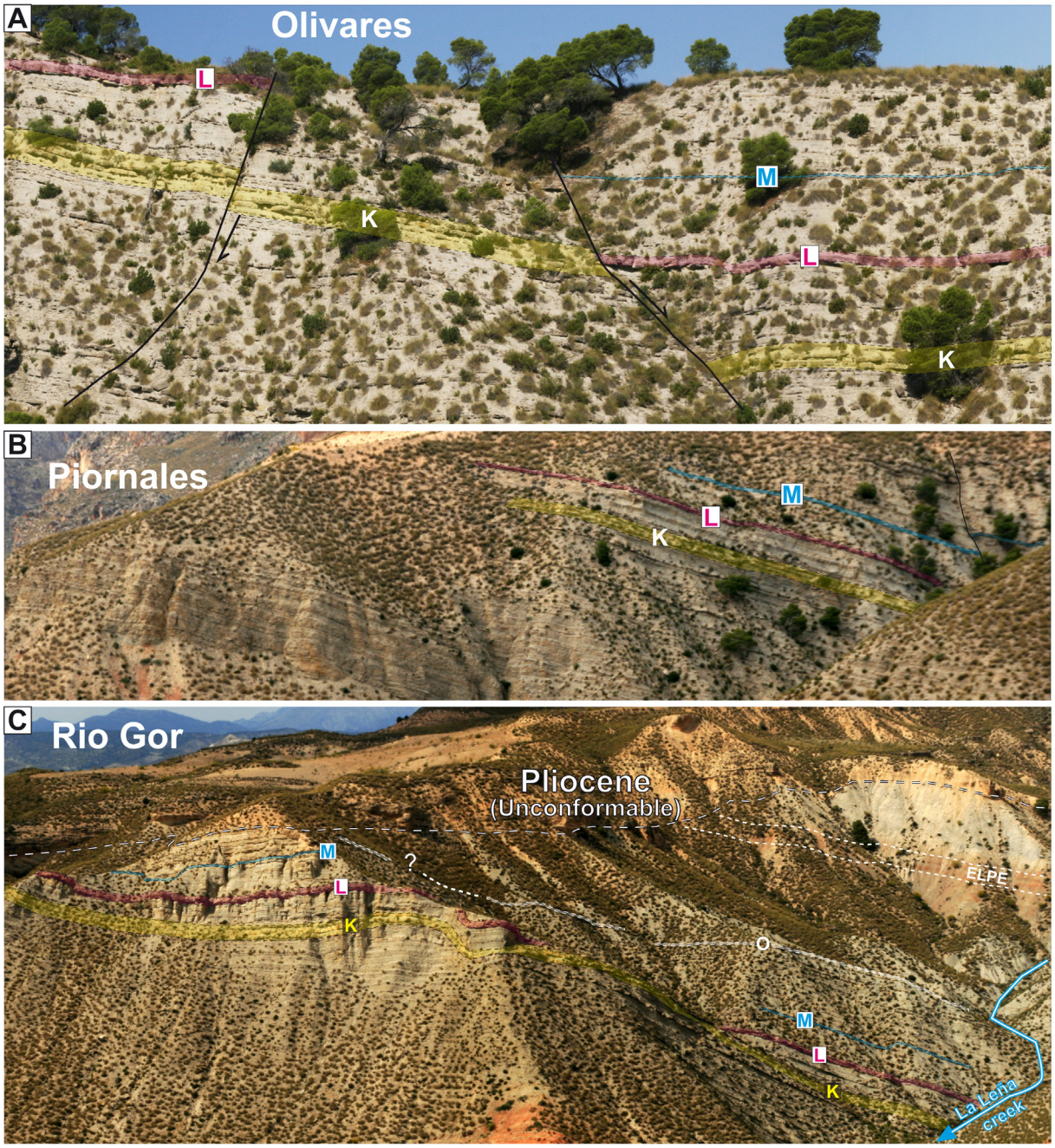

Fig. 7. General field views of the three sections of the Olivares Formation studied in this paper with indication of reference calcarenites K, L and M in all of them.

approximately, to the lower and upper parts of the unit in the description of Rodriguez-Tovar et al. (2020), and Members 3 and 4 to the transitional part of the same authors.

Member 1 is 23 m thick and is mostly composed of very thin- and thin-bedded *Microcodium*-rich calcarenites with subordinate marly interbeds (Fig. 6A), although near its base it contains a couple of medium-bedded calcarenites. The trace fossil association of this member belongs to the *Ophiomorpha rudis* subichnofacies of the deep marine *Nereites* ichnofacies (Rodriguez-Tovar et al., 2020). The member rests abruptly but conformably on red marls of the Capas Rojas Formation of the early/middle Danian P1 Biozone (Figs. 2B, 5A).

Member 2 is 35 m thick and evolves gradually from the underlying Member 1. It is also mainly made up of very thin- and thin-bedded calcarenites but, unlike Member 1, it includes numerous medium- and

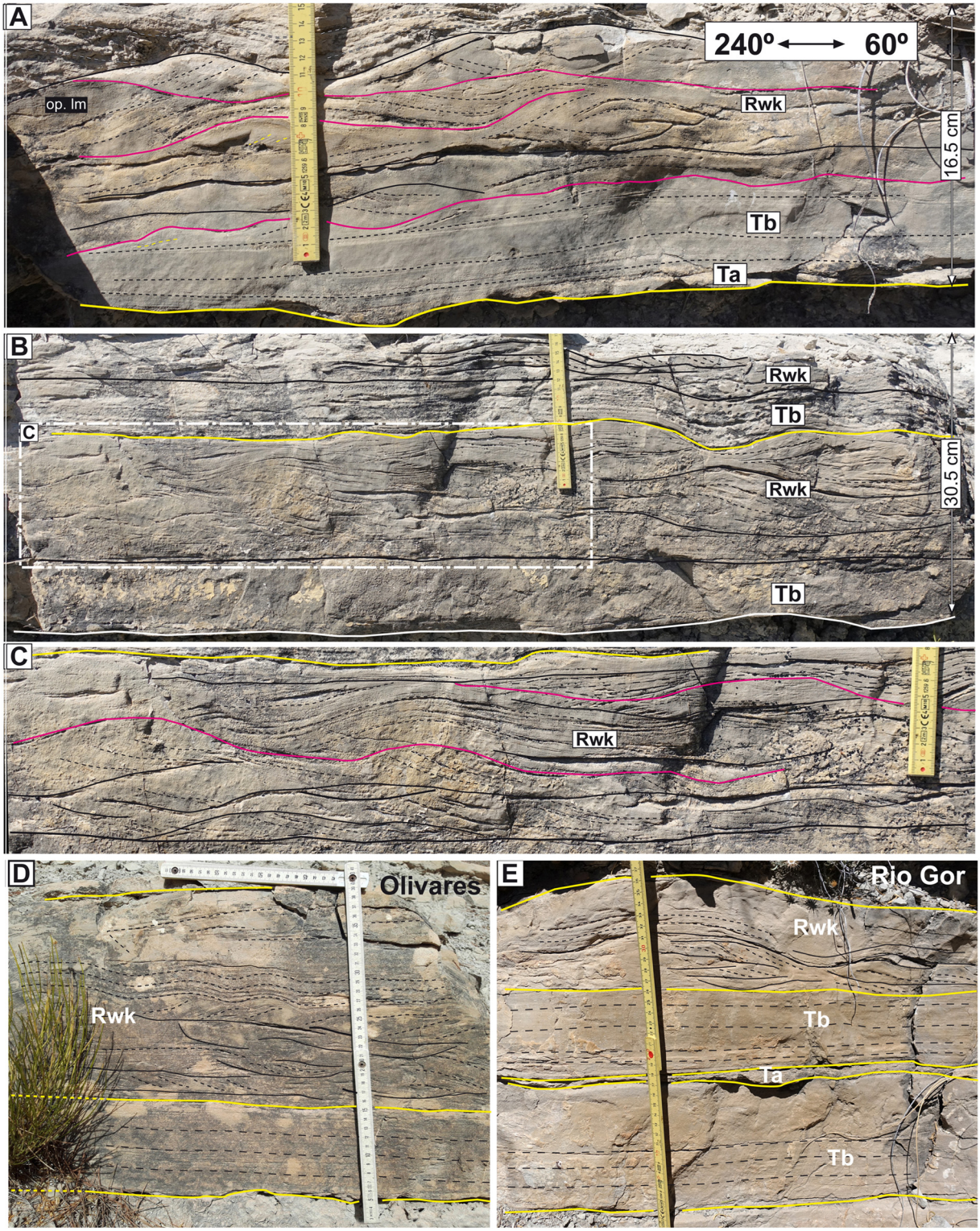

Fig. 8. (A, B, C) Representative examples of internal laminations of medium-bedded calcarenites from Member 2 of the Olivares section; purple lines in A and C highlight some set boundaries. (D, E) A comparison of the internal lamination of two coeval thick-bedded calcarenites from the Olivares and Rio Gor section, respectively. Ta, Tb: divisions of the Bouma sequence; Rwk: reworked parts of the calcarenites. Explanation within the text.

thick-bedded calcarenites (Fig. 6B), marked F–K in Fig. 5. Those coded F, G and J correspond to individual strata, while H, I and K consist of groups of two or three beds. In addition to such lithological difference, the trace fossil association of Member 2 pertains to the *Paleodictyon* subichnofacies of the *Nereites* ichnofacies, which denotes somewhat deeper conditions than the subichnofacies of Member 1 (Rodriguez-Tovar et al., 2020).

Member 3 is 19 m thick and is dominated by calcisiltites and marls, with a lesser proportion of thin-bedded *Microcodium*-rich calcarenites and a few beds of hemipelagic limestones (Fig. 6C). Due to the predominance of more friable deposits, Member 3 stands out in the landscape as a recessive interval (Figs. 5B, 6C). It is therefore somewhat paradoxical that Member 3 includes, near its middle part, the thickest calcarenite of the Olivares Formation (1.65 m; reference bed L in Figs. 5B, 6C). Trace fossils observed in the calcisiltites are not diagnostic (see below).

Member 4 is 22 m thick and, similarly to Member 2, contains calcarenites of a wide range of thicknesses, from very thin up to a maximum of 90 cm (bed O in Fig. 5B). Likewise, trace fossils in Member 4 are readily attributable to the *Nereites* ichnofacies. However, the calcarenites of Member 4 have a more varied composition than those of Member 2: most of them are still *Microcodium*-rich, but others are either bioclastic or have a mixed nature, the former rich in broken and whole tests of planktonic foraminifera, the latter characterized by alternating bioclastic and *Microcodium*-rich layers (see below). In addition to that, the proportion of marls in Member 4 is higher than in Member 2.

Planktonic foraminifera information demonstrates that the bulk of Member 1 is ascribable to the late Danian P2 Zone, Member 2 to the late Danian-lowest Selandian P3 Zone and Members 3 and 4 to the Selandian P4 Zone (Fig. 5A). The top of Member 4 (and thus of the Olivares Formation) is situated about 40 m below the ELPE and, therefore, roughly in the middle part of the Selandian (Fig. 2B). It can hence be concluded that the Olivares Formation comprises the late Danian-early Selandian interval, a time span of about 2.5 Ma according to the chronostratigraphy of Wade et al. (2011) (Fig. S1).

4.2.3. Sedimentary features of medium and thick bedded calcarenites

Medium- and thick-bedded calcarenites of the Olivares Formation, which are abundant in Members 2 and 4 and occasional in Member 3, provide important genetic clues. For that reason, they are described before the other lithologies in the unit.

The thickest calcarenite beds are laterally extensive. Beds K, L and M, for example, can be traced across the entire 2.5 km width of the

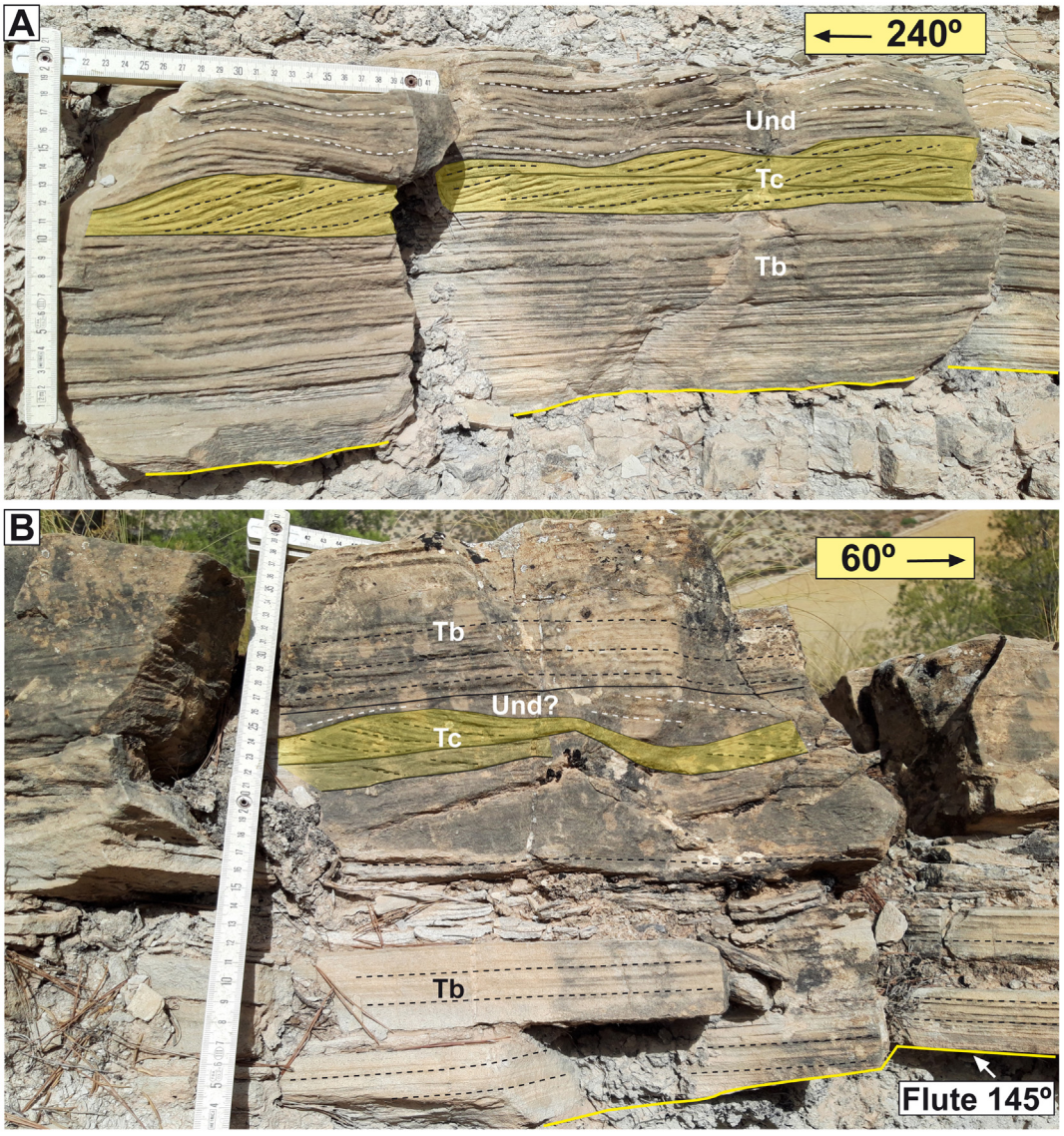

Fig. 9. (A, B) Internal laminations of medium-bedded calcarenites from Member 4 in the Olivares section. Note that the cross-laminated set (Tc) in A indicates palaeocurrents opposite to those in B, and that palaeocurrents from flutes (not shown) in B are near perpendicular to those of the cross-laminated sets. Note also the well-defined laminations in both beds. Tb, Tc: divisions of the Bouma sequence; Und: undulating lamination. Explanation within the text.

outcrops, from the Olivares section to about 0.5 km to the SE of the Rio Gor section. These beds can be readily identified in the three studied sections, and in parts of the intervening landscape, because they occur at the base, middle and top, respectively, of the recessive Member 3 (Fig. 7A–C). Other medium and thick beds likely have similar lateral extension, a possibility that cannot be verified due to outcrop constraints. In the Rio Gor section, for instance, bed O from the top of Member 4, can be followed in the landscape for hundreds of meters without any perceptible change in thickness (Figs. 5B, 7C). The real extension of this bed, however, cannot be ascertained because the upper part of Member 4 is eroded away or poorly exposed in the other two studied sections (Fig. 7A, B).

As a rule, beds thicker than 15 cm have erosional bases, some of them decorated with flute marks (Fig. S4A, B). These beds usually contain three stacked divisions that, in the thicker of them, can be repeated in the vertical (Fig. 8). The lower division (not always present) is up to 5 cm thick and is composed of normally graded granule- or very coarse sand-grade grains (Fig. 8A, E). The middle division is 5–10 cm thick and consists of parallel laminated calcarenites (Fig. 8A–E) that, in plan-view exposures, exhibit parting lineation (Fig. S4B). The features of these two divisions, coupled with the basal erosional surface, are thus akin to the Ta and Tb divisions of the Bouma sequence, respectively.

The upper division is characterized by cross-laminations but is very different from the Tc division of the Bouma sequence. In effect, the lower boundaries of cross-laminated sets are undulating, not straight or smoothly curved as those of the Bouma Tc division. Besides, cross-laminations, as a whole, are bidirectional, individual cross-laminae may drape over lower set boundaries, even on adjacent convex-up and concave-up parts of them. Also, the laminae usually rest tangentially on the set boundaries and the laminations are never convoluted (Fig. 8A–E). Therefore, for descriptive purposes, the upper division of

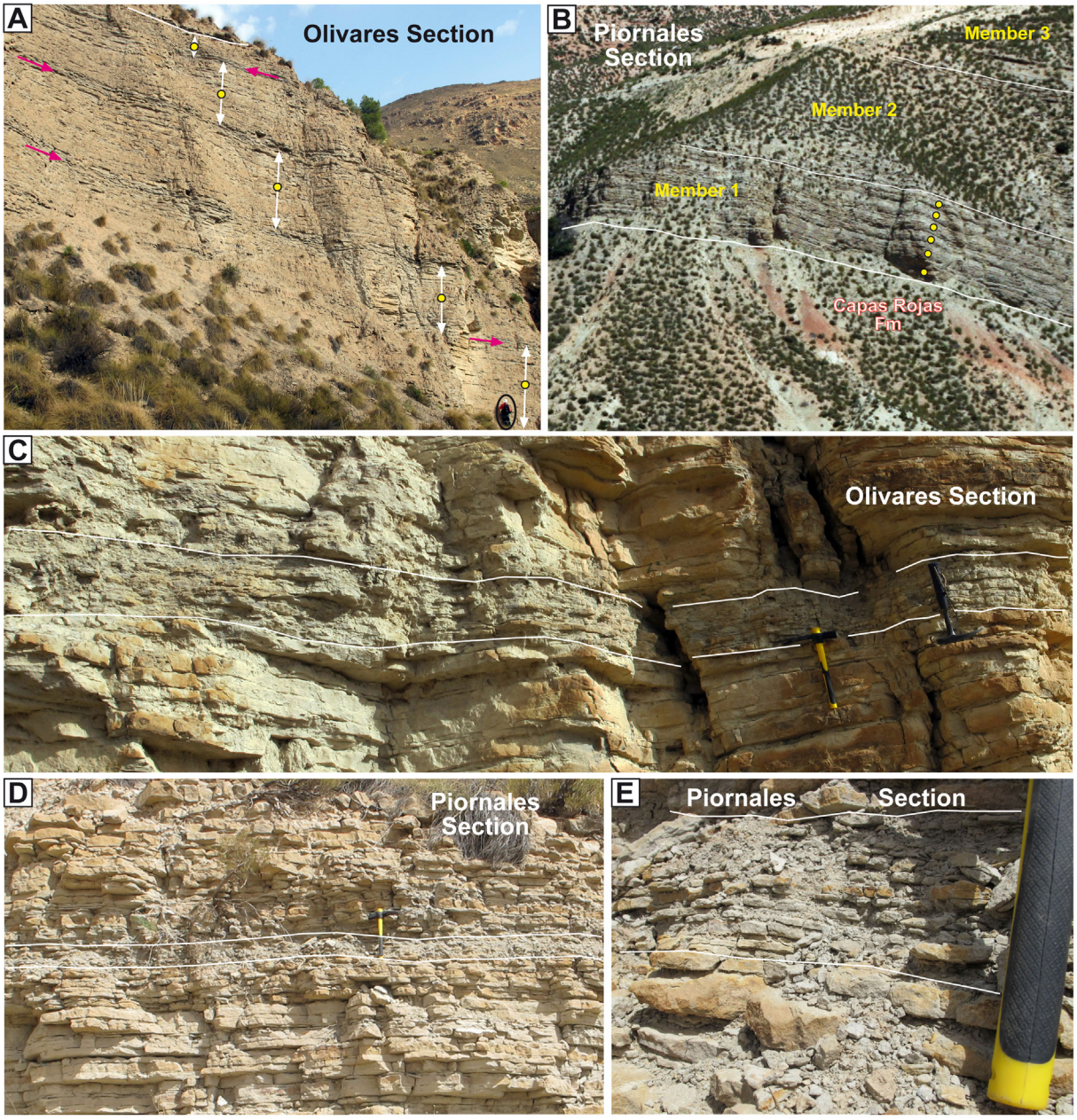

Fig. 10. (A, B) General views of Member 1 of the Olivares Formation in the Olivares and Piornales sections, showing 3–4.5 m-thick packages mostly composed of very thin- and thin-bedded *Microcodium*-rich calcarenites (yellow dots and/or double-headed white arrows) separated by 10–30 cm thick intervals of very thin calcarenite/marl alternations (pink arrows in A; encircled geologists at the bottom right of the image gives scale). (C, D, E) Close-ups of the intervals of very thin calcarenite/marl alternations sandwiched between the calcarenite packages.

the studied calcarenites has been labeled Rwk (reworked). Interestingly, in reference bed K, the thickness of the Rwk division is greater in the Olivares section than in the Rio Gor section (Fig. 8D, E).

All the examined thin sections from samples of the Ta and Tb divisions contain *Microcodium* aggregates, in addition to which some also contain ooids, miliolids, quartz grains and/or intraclasts (Figs. 3A, S5A, B). The ooids must have been derived from lower Lias and/or Dogger carbonate units of the Subbetic Zone, which are rich in them (Vera, 2004). Some of the intraclasts contain calpionellids (Figs. 3A, S5A), which in the Subbetic Zone only occur in Berriasian limestones (e.g., Comas et al., 1970, 1973). Instead, thin sections from reworked intervals are mostly composed of fragmented *Microcodium* grains with sizes ranging from 80 to 150 μm, and poorly defined grain segregation (Figs. 3B, S5C).

A significant exception to the above has been observed in the Olivares section, in a couple of beds of Member 4 that stand out due to their very prominent laminations (Fig. 9A, B). In these two beds the Tb parallel-laminated calcarenites are not overlain by Rwk divisions, but by unidirectional cross-laminated sets clearly created by current ripples or small dunes. In one of the beds the cross-laminated set is overlain by undulating laminations (Und in Fig. 9A). It is tempting to assimilate such cross-laminated sets to the Tc division of the Bouma sequence, but the assimilation faces two obstacles: one, the cross-laminations of the bed in Fig. 9A indicate palaeocurrents toward 240°E, while those in the bed in Fig. 9B are toward 60°E, practically opposed to each other; two, flute marks from the base of the latter bed indicate palaeocurrents toward 145°E, almost at right angle to those of the laminations (Fig. 9B). These facts indicate different currents, one responsible for the flutes and probably also for the parallel laminations, others for the opposite directed cross-laminations.

Thin sections reveal that these, and other beds with prominent laminations (see below), have a mixed composition, with laminae rich in *Microcodium* grains alternating with others dominated by reworked tests of planktonic foraminifera (Fig. S6A). The prominent laminations of these beds very likely result from the differential weathering of these laminae.

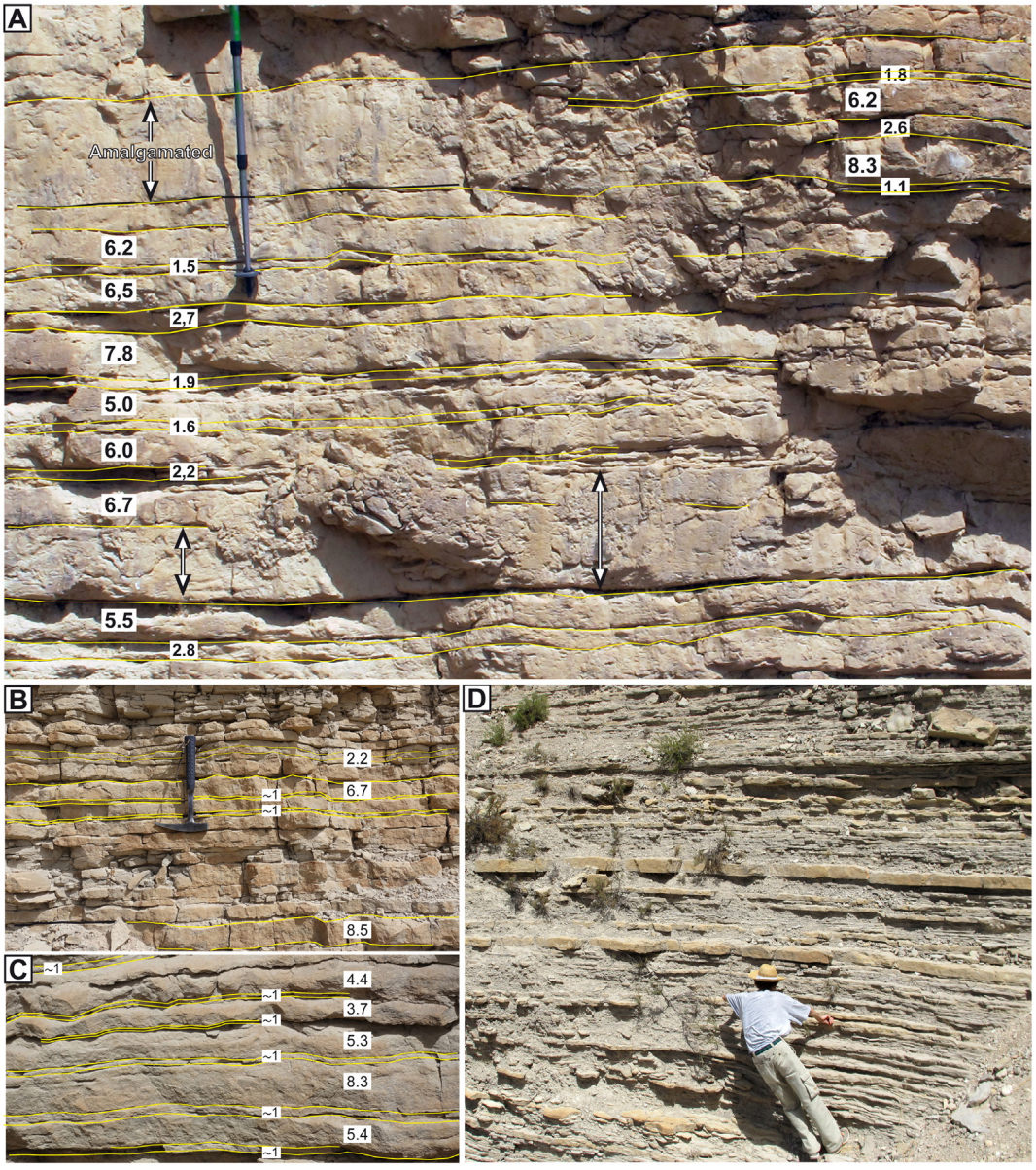

Fig. 11. Field views of representative segments of Member 1 of the Olivares Formation in the three studied sections. (A) Olivares section: frequent alternation of very thin- and thin-bedded calcarenites (numbers give bed thicknesses in cm), amalgamation of individual beds into thicker strata (double-headed arrows), and near absence of marls. (B, C) Piornales section: stacked very thin- and thin-bedded calcarenites, some with undulating tops, separated by extremely thin marly partings. (D) Rio Gor section: predominance of very-thin and thin-bedded calcarenites separated by thin marly interbeds.

4.2.4. Sedimentary features of thin- and very thin-bedded calcarenites

Thin and very thin-bedded calcarenites are predominant in Member 1 of the Olivares Formation and subordinate in the other three members. Therefore, the description of these calcarenites is mainly based on data from Member 1, where their features are not distorted by the "noise" introduced by other lithologies.

Member 1 exhibits significant differences in the three sections analyzed in this study, the most important of which concerns the amount and distribution of marls. Thus, in the Piornales and the Olivares sections marls are only abundant, intermingled with very thin calcarenites, within 10–30 cm thick intervals intercalated between 3–4.5 m-thick packages of calcarenites almost devoid of them. Five of these packages are recognized in the Olivares section and six in the Piornales section (Fig. 10).

The scarcity of marls within the packages is most severe in the Olivares section, where the marly interbeds are extremely thin and

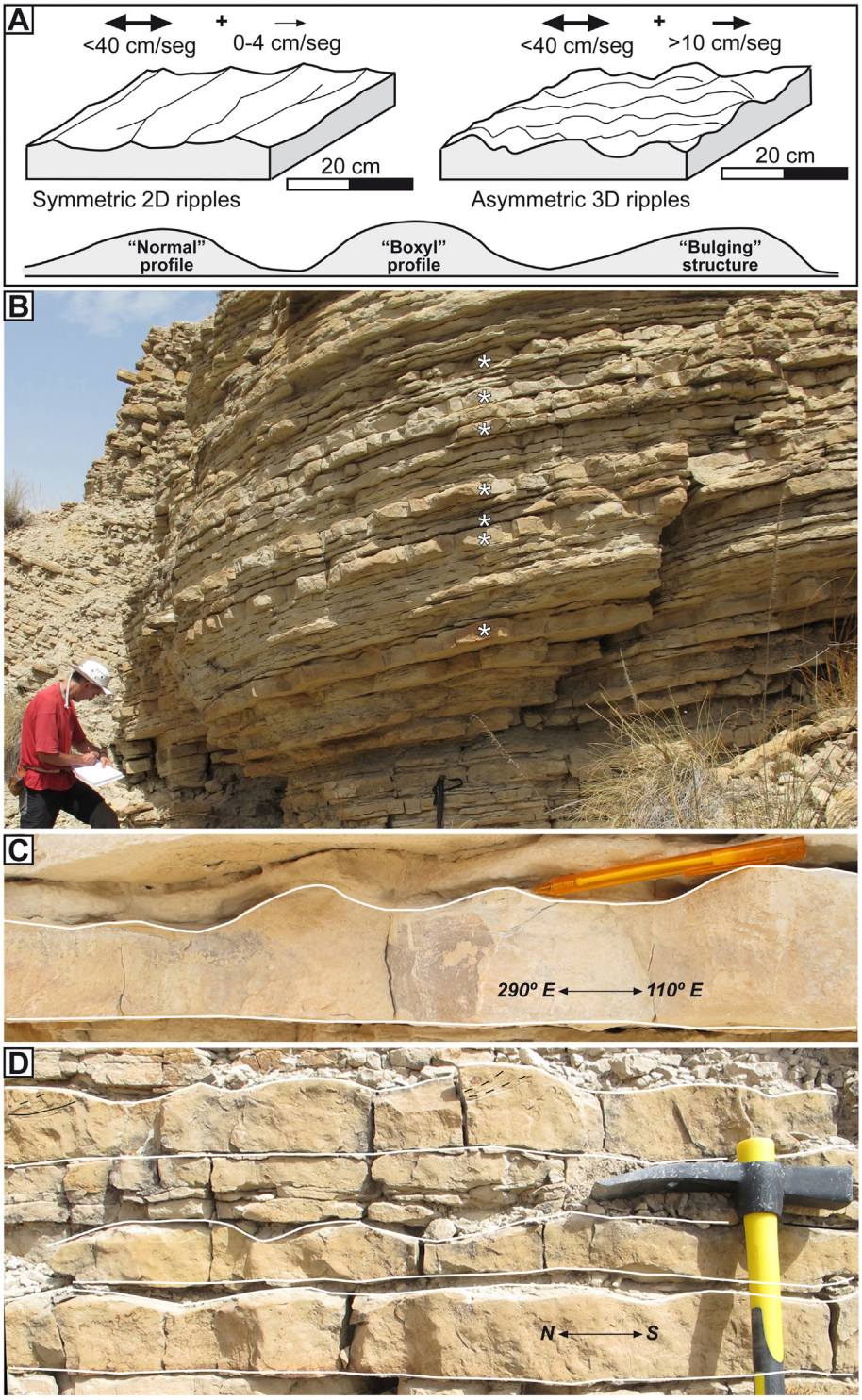

Fig. 12. (A) Line drawings of ripples generated in a flume by oscillatory (symmetric) and combined flows (asymmetric), and profile variations in asymmetric small-scale ripples (modified from Table 2 and Fig. 5 of Dumas et al., 2005). (B) General view of part of Member 1 in a three-dimensional exposure of the Piornales section; white asterisks indicate beds with undulating top surfaces. (C, D) Close-ups of two parts of the exposure with almost perpendicular orientations, showing undulating top surfaces. Explanation in the text.

often absent, so that the very thin calcarenite beds amalgamate into thicker strata (Fig. 11A). A rhythmic alternation of thin (3.7–8.3 cm) and very thin-bedded (1–2.8 cm) calcarenites is common at Olivares (Fig. 11A), and can be observed occasionally at Piornales (Fig. 11C). Instead, bed amalgamation is infrequent in the Piornales section, where most individual beds are demarcated by thin but laterally continuous marly interbeds (Fig. 11B, C).

A substantial number of thin-bedded calcarenites of Piornales exhibit rippled tops in profile, but the absence of plan-view exposures makes it difficult to establish the precise morphology of their parent bedform. However, based on flume experiments, Dumas et al. (2005) developed criteria to distinguish profiles of ripples generated by oscillatory and combined flows. These authors found that pure oscillatory currents create symmetric, two-dimensional (2D) ripples with smooth regular profiles, whereas combined-flows create asymmetric, three-dimensional (3D) ripples that have broad and round crests of different shapes ("normal", "boxy" or "bulging") depending on the intensity of turbulent eddies at the lower ends of ripple stoss sides (Fig. 12A). As shown in Fig. 12B–D, individual ripples at the top of thin-bedded calcarenites at Piornales have broad and round crests that closely resemble those described by Dumas et al. (2005). Further, the outcrop at Piornales offers exposures with almost perpendicularly orientations (Fig. 12B), and the fact that bed profiles are nearly identical irrespectively of their orientation (Fig. 12C, D) strongly argues in favor of asymmetric 3D ripples (cf., Fig. 12A).

In contrast with the above, in the Rio Gor section thin and very thin-bedded calcarenites alternate with marly interbeds a few mm to cm thick throughout most of Member 1 (Fig. 11D). Consequently, bed amalgamation is seldom seen at Rio Gor. Likewise, marl-rich intervals similar to those separating larger calcarenite packages at Olivares and Piornales have not been detected. In this section a large number of calcarenite beds have undulating tops with shapes resembling those of the Piornales section, although with less pronounced reliefs. Less frequently, examples of symmetric ripples have also been observed on a few bedding surfaces (Fig. S4E, F).

Internal laminations are not visible in the very-thin bedded calcarenites but can be observed, although usually somewhat diffuse, in some thin beds of the Piornales and Rio Gor sections (Fig. 13A–F). These include a few examples of parallel-laminated intervals akin to the Bouma Tb interval (Fig. 13A), but most are similar to those of the

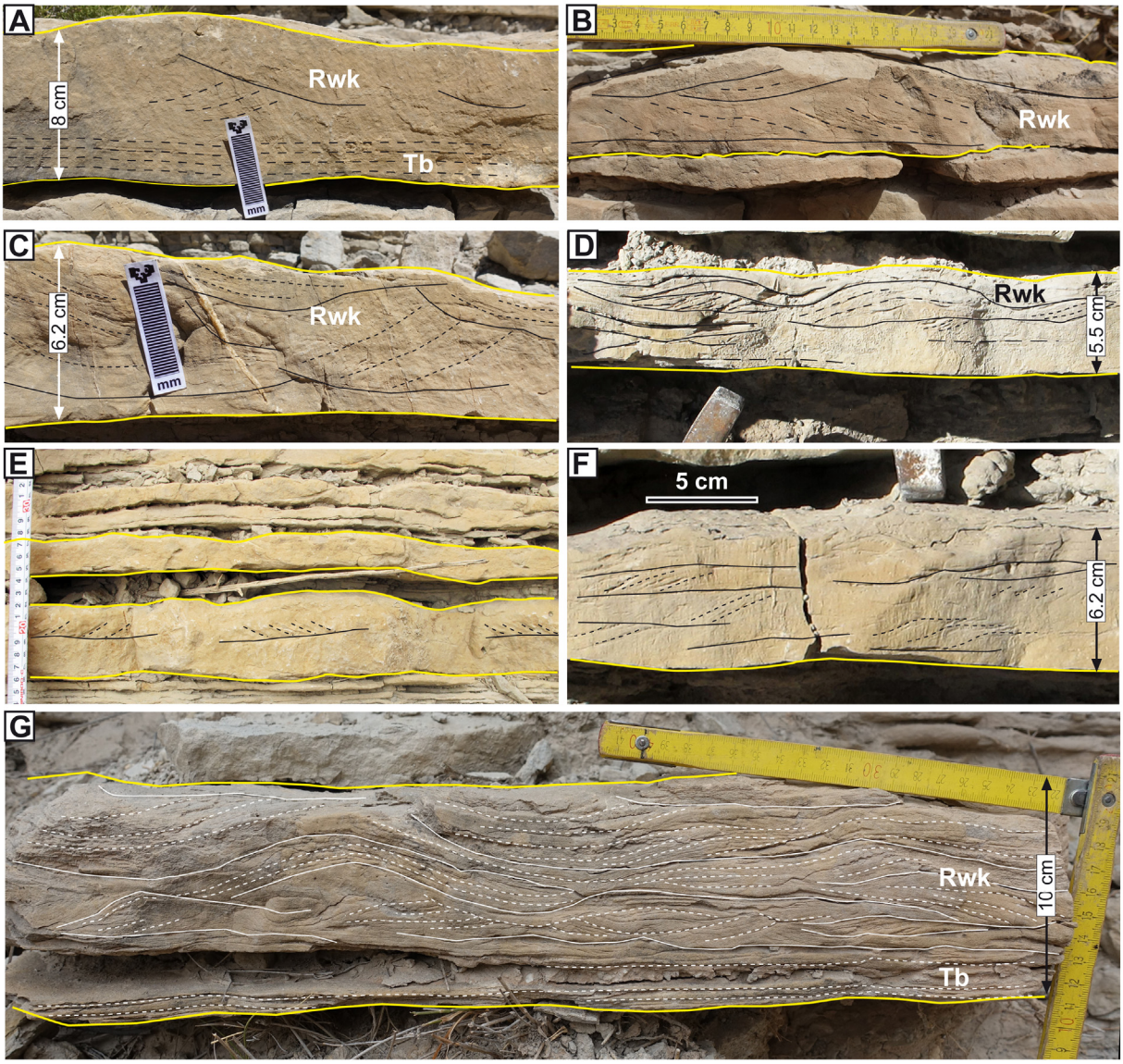

Fig. 13. Representative examples of internal laminations of thin-bedded calcarenites from the Rio Gor section, all of them with similar orientation. (A–D) Beds dominated by reworked laminations (Rwk), some of them underlain by a parallel laminated zone akin to Bouma's Tb interval. (E–F) Beds with current ripple laminations; note the opposite orientations in E. (G) Bed from Member 4 showing prominent laminations typical of Rwk intervals. Explanation within the text.

reworked cross laminations of medium- and thick beds, having variable orientations and concave-up or undulating bounding surfaces (Fig. 13A–D). Cross-laminated sets with flat lower bounding surfaces also exist, some of them being bidirectional (Fig. 13E) and others unidirectional (Fig. 13F).

Thin sections of thin- and very thin-bedded calcarenites are almost exclusively composed of *Microcodium* grains of a narrow size range (100–250 μm). Neither graded bedding nor clear grain segregation are perceptible (Fig. 3B). The poorly defined internal lamination in these calcarenites likely results from the near homogeneous size and distribution of their *Microcodium* prisms.

Thin sections also demonstrate that a number of medium and thin-bedded calcarenites of Member 4 have a mixed composition, with the characteristic alternation of laminae rich in *Microcodium* grains and planktonic foraminifera tests (Fig. S6A). Similar prominent laminations, resulting from differential weathering, have also been observed in reworked intervals of medium and thick bedded calcarenites of Member 4 (Figs. 9, 13G).

4.2.5. Sedimentary features of calcisiltites

Calcisiltites are the main component of Member 3. They occur in plane-parallel beds 1.5–5 cm thick, separated by marly interbeds, usually (sub)millimetric but sometimes up to 5 cm thick (Fig. 14A, B). They commonly intercalate thin-bedded *Microcodium*-rich calcarenites (arrowed in Fig. 14A), a few beds of whitish limestones (arrowed in Fig. 14B) and, as mentioned above, the thickest *Microcodium*-rich calcarenite of the Olivares Formation (reference bed L in Figs. 5B, 6C).

In the field the calcisiltites seem to be structureless, but polished hand samples and thin sections demonstrate that they are internally bioturbated in variable degrees. In mildly bioturbated cases two different lithologies can be distinguished, one consisting of dark mudstone/wackestone with small planktonic foraminifera, the other mainly composed of small *Microcodium* grains (25–60 μm) dispersed in a dark matrix (Fig. 14C). Both lithologies, however, become mixed-up when bioturbation is pervasive (Fig. 14D). The bioturbation consists of cylindrical galleries infilled with *Microcodium* grains bordered, totally or partially, by dark foraminiferal mudstone/wackestones (Fig. 14E, F). Such

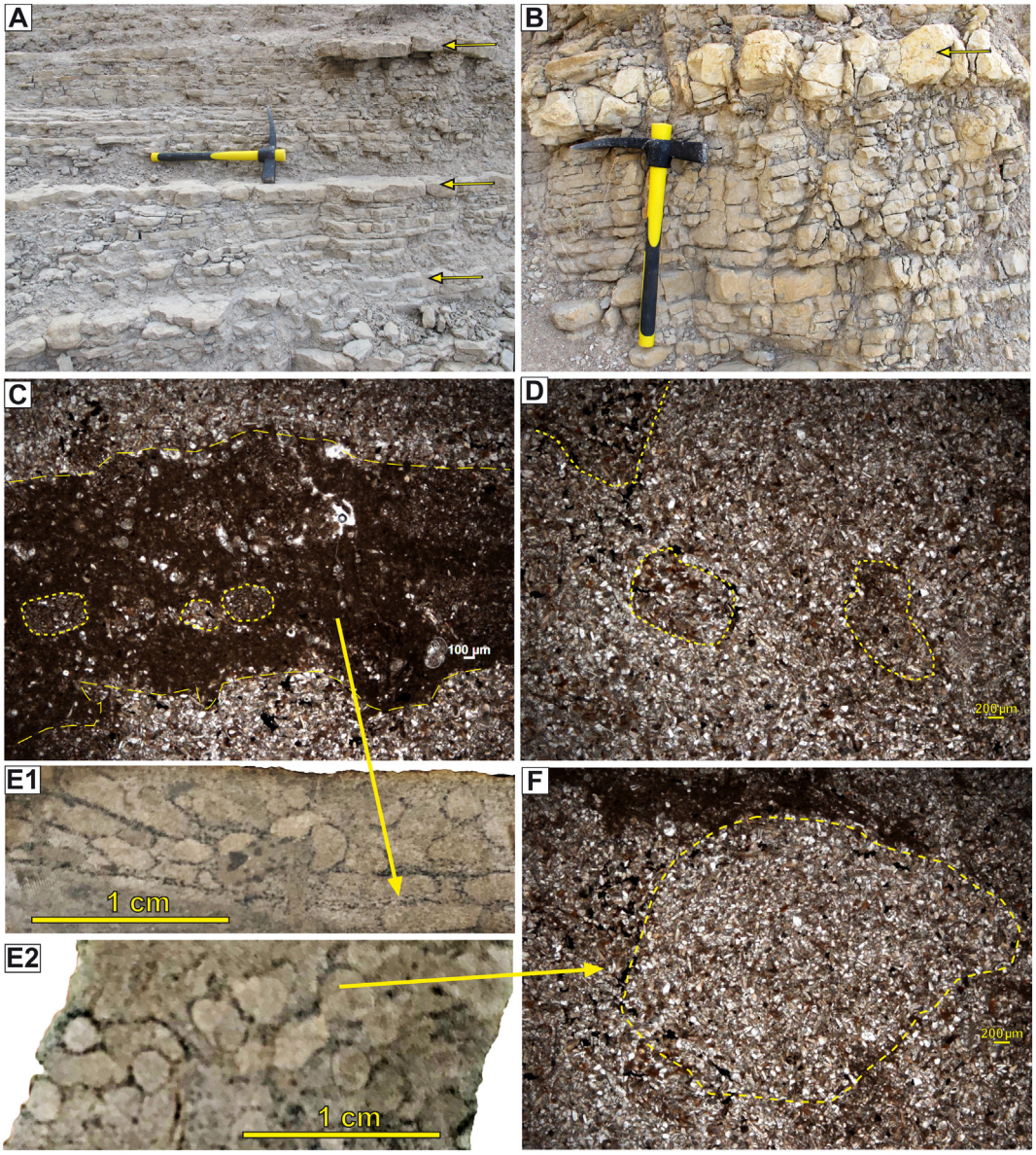

Fig. 14. (A, B) Close-ups of representative segments of Member 3 of the Olivares Formation showing predominance of calcisiltites with intercalated thin-bedded calcarenites (arrowed in A) and a hemipelagic limestone bed (arrowed in B). (C–F) Thin section micrographs of calcisiltites and polished slabs from which the thin-sections were acquired. (C, E1) Alternating layers of dark mudstone with small foraminifera and others rich in silt-sized *Microcodium* grains, not entirely mixed up by bioturbation. (D, F, E2) More bioturbated calcisiltites, in which the dark mudstone layers have been almost entirely eliminated. Explanation within the text.

galleries were likely produced by worms feeding on dispersed organic matter of the dark mudstone/wackestones.

4.2.6. Other lithologies

Gray marls, bioclastic calcarenites and whitish limestones complete the lithological catalog of the Olivares Formation. Gray marls are nondescript mixtures of clay and carbonate, part of which are the tests of foraminifera and calcareous plankton. They occur intercalated within other lithologies of the unit, in very low proportion in Member 1, low in Member 2, and moderate in Members 3 and 4.

Bioclastic calcarenites are packstones largely composed of reworked planktonic foraminifera tests with a small proportion of mud-grade fraction (Fig. S6B). They only occur in Member 4, as thin- and medium-bedded strata similar in field appearance to *Microcodium*-rich calcarenites, from which they can only be distinguished in thin sections.

Whitish limestones have been detected only in Member 3 of the Rio Gor section, where two beds, each about 10 cm thick, are intercalated within the calcisiltites (Figs. 5B, 14B). They are wackestones, with small-sized planktonic foraminifera and other unidentified microfossils dispersed in a mud-grade matrix (Fig. S6C).

4.3. The Capas Rojas Formation in the Alamedilla sector

4.3.1. Location and data base

In the Alamedilla sector the entire upper Cretaceous-lower Eocene succession belongs to the Capas Rojas Formation. Outcrops of the unit are restricted to the northern and southern flanks of a wide gentle synclinorium, near the villages of Alamedilla and Pedro Martínez, respectively (Fig. 1C). Those to the south of Alamedilla are best exposed and have therefore received more attention. In fact, the type section of the Capas Rojas Formation, frequently called "Alamedilla section" (Vera et al., 1982), is situated in this sector along the Rambla Valencianos (Figs. 2A, 15). Previous studies in this section mainly focused on the late Cretaceous (e.g., Linares, 1977; Arz, 2000), early Eocene (Gonzalvo and Molina, 1998) and, especially, the Paleocene-Eocene boundary intervals (e.g., Arenillas and Molina, 1996; Lu et al., 1996, 1998; Monechi et al., 2000; Alegret and Ortiz, 2009; Alegret et al., 2009, 2010). In contrast, the Danian-Selandian interval, which is crucial for the purposes of this study, has been largely overlooked to date. For this study the Valencianos, Barranco and Dirt track, sections, previously studied by Pujalte et al. (2014b, Fig. S7), were revisited and resampled. In addition, the planktonic foraminifera data reported by Martínez-Gallego (1977) from the Valencianos and two other sections of the Alamedilla sector, San Jose and Cejo 1, as well as the data reported by Pujalte et al. (2014b) from the Cejo 2 section, have been taken into account (Figs. S7, S8).

4.3.2. The late Maastrichtian-early Ypresian interval

In the Alamedilla sector the late Maastrichtian-early Ypresian interval of the Capas Rojas Formation is composed of four informal units of contrasting colors (Fig. 16A, B), a circumstance that facilitates their mapping on Google Earth satellite images (Fig. 16C). Unit 1 in the Valencianos section is 44 m thick and is mostly made up of marls of pink color. Unit 2 is 28 m thick and it is dominated by marls of a deep red color with a limestone intercalation about 1 m thick (Fig. 16B). Our foraminiferal data indicate that the entire unit 1 and the lower 15 m of unit 2 pertain to the latest Maastrichtian *A. mayaroensis* biozone, and the remainder 13 m of unit 2 to the middle Danian (P1c subzone, Fig. 16B). The absence of the Po, P1a and P1b subzones in the middle part of unit 2 entails a hiatus of about 3 Myr (Fig. S1), which encompass the K/Pg boundary. However, no hard-ground or other indications of sedimentary discontinuity have been observed in the field. Thus, the upper Maastrichtian-middle Danian successions at the Valencianos and Rio Gor sections are very similar, except for the intercalated limestone in the former section and of calciturbidites in the latter (cf. Figs. 2 and 16A).

Unit 3, which overlies abruptly but concordantly unit 2, is 16 m thick in the Valencianos section and it is composed almost exclusively of gray marls (Fig. 16A, B). Samples from the lower part of the unit contain, among other planktonic foraminifera, *Gl. pseudomenardii* and *A. soldadoensis*, their co-occurrence demonstrating the late Thanetian P4c biozone (Fig. 16B). The absence of P2 to P4b biozones entails the existence of a ca. 5.4 Myr long hiatus at the boundary of units 2 and 3, which is also recognizable in the Barranco, Dirt track and Cejo 2 sections (Fig. S7). The cross-sections in Fig. 16D, E demonstrate that the hiatus at the base of unit 3 is linked to an irregular disconformity with a relief of 15 m in the Barranco section and 3.5 m in the Cejo 2 section. A bed-to-bed correlation among sections could potentially unveil additional minor disconformities. However, achieving such a correlation proves challenging because the marly composition of the succession favors the proliferation of bushes, as exemplified by the Cejo 2 section (Figs. S7B, C).

Unit 3 is capped by a comparatively thin horizon (≈2 m) of marls and marly clays of a conspicuous deep red color that, as reported by

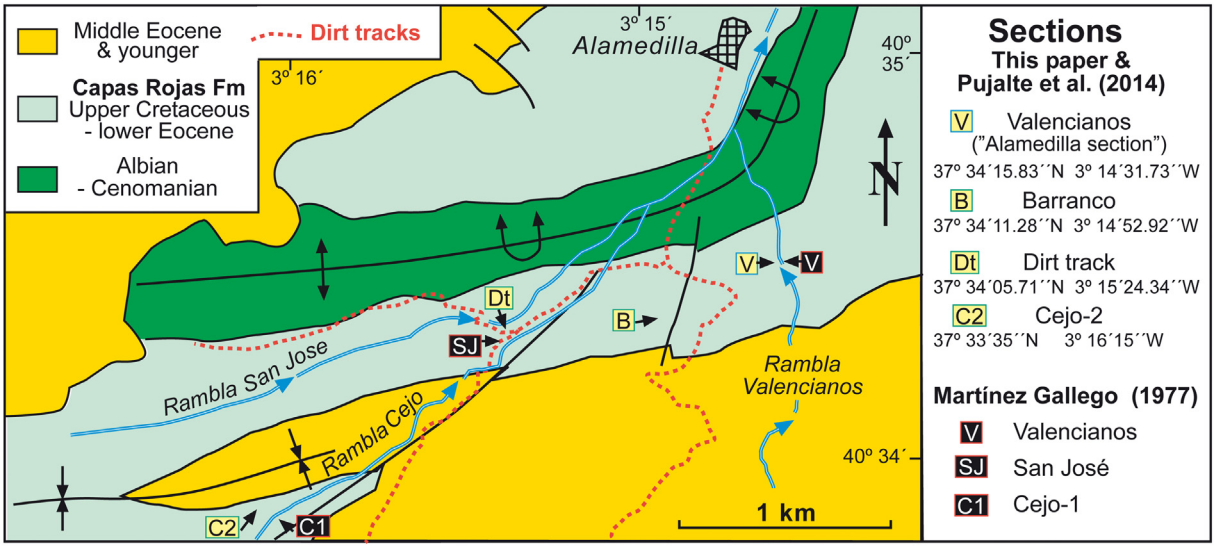

Fig. 15. Geological map of the of the Alamedilla sector (modified from Díaz de Neira et al., 1988; situation in Fig. 1C), with location of the sections analyzed by Martínez-Gallego (1977) and by Pujalte et al. (2014b), the latter revisited in this study.

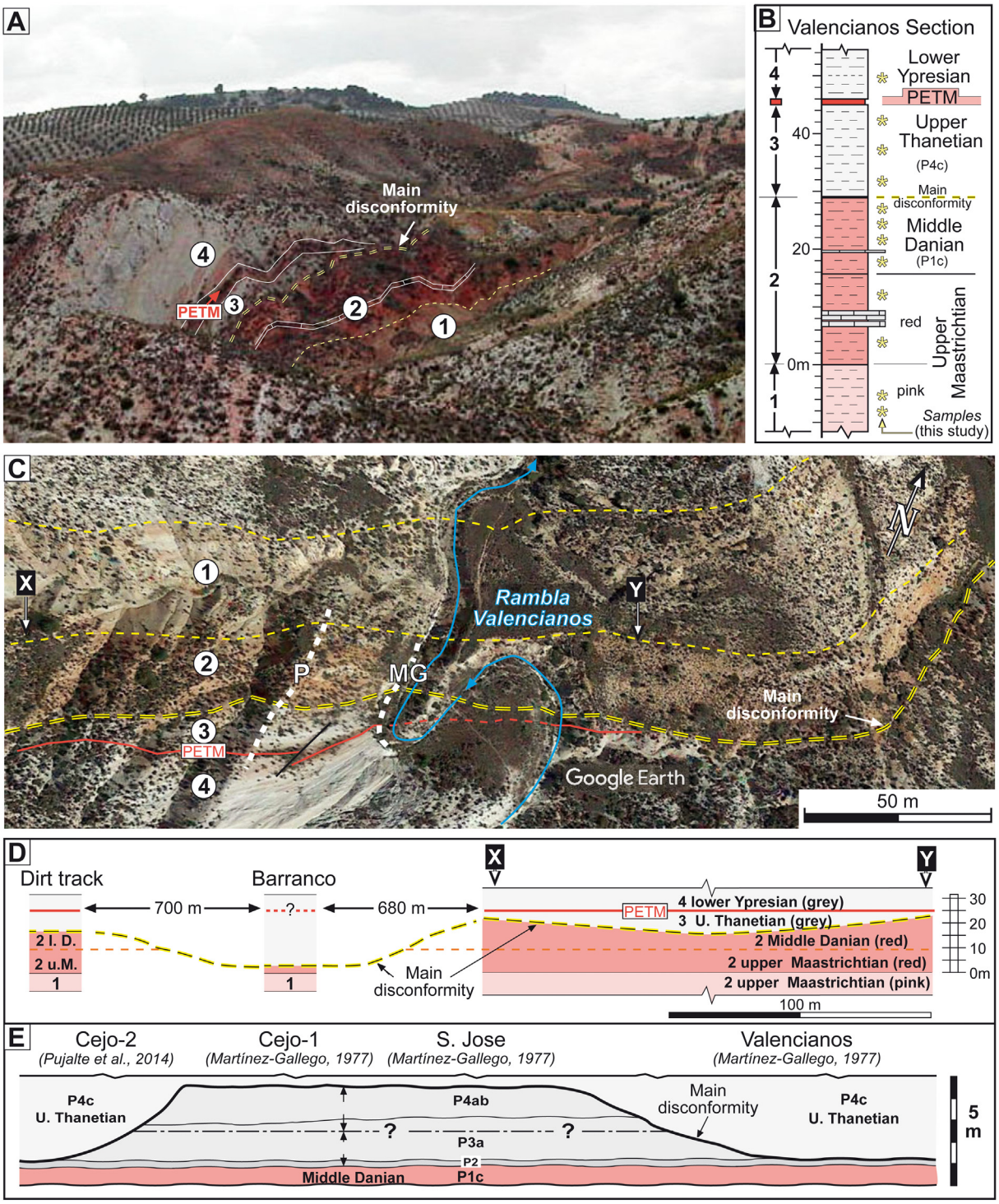

Fig. 16. Alamedilla sector. (A) Field view of the upper Maastrichtian to lower Ypresian segment of the Valencianos section. (B) Log and planktonic foraminifera zonation of the late Maastrichtian-Paleocene interval of the section with indication of the four lithologic units (differentiated by colors) and location of samples analyzed in this study. (C) Google Earth color image around the Valencianos creek with lines separating the four units differentiated in this study; the broken white lines MG and P indicate the transects sampled by Martínez-Gallego (1977), by Pujalte et al. (2014b) and in this study. (D) Cross-section created by the correlation of the transect X-Y in panel C and data from the Barranco and Dirt track sections. (E) Correlation of the Cejo 2 section and the three sections analyzed by Martínez-Gallego (1977), their thickness and planktonic foraminifera data being shown in Fig. S8.

previous authors (see above) records the PETM (Fig. 16A–C). The PETM also occurs in the Dirt track section, but is absent in the Barranco, Cejo 2 and Pedro Martínez sections (Fig. S7A). The PETM grades up into an alternation of gray marls and limestones dated as early Ypresian (unit 4, Fig. 16), the study of which is beyond the purposes of this paper.

The results from the high resolution sampling of Martínez-Gallego (1977) in the Valencianos section are comparable to those described above, with the only difference of the recognition by this author of a 30 cm thick interval belonging to P2 biozone. The other two sections analyzed by Martínez-Gallego (1977), Cejo 1 and S. Jose, contain records of P2, P3 and P4ab biozones, all of them with small thicknesses (Fig. S8). In any case, although reduced, the preservation of these biozones proves that sedimentation in the Alamedilla sector was neither continuous nor homogeneous during the Danian-Selandian interval.

4.4. The late Maastrichtian–early Palaeogene interval in the eastern and western Subbetic Zone

Data from the geological literature indicate that the characteristics of upper Maastrichtian-Paleocene successions in both the western and eastern parts of the Subbetic Zone are comparable to those described above. *Microcodium*-rich calcarenite units, in particular, are scattered throughout the Subbetic Zone, the best studied being the Majalcorón Formation (Fig. 1A, C). According to Vera et al. (2004) and Molina et al. (2006), outcrops of this Formation are limited to a comparatively small area to the south of the Alcalá la Real village (Fig. 1C). The unit is 56 m thick in its type section, its thickness decreasing to the east, west and south. It mostly consists of well-stratified, medium to thick-bedded calcarenites with lesser thin intercalations of marls and wackestones (Fig. S9A, B). The calcarenites are mostly (40–90 %) composed of *Microcodium* grains and aggregates. The remainder components are quartz grains, bioclasts and plant remains. The unit is underlain and overlain by marls rich in planktonic foraminifera and calcareous nannofossils. Martínez-Gallego and Roca (1973) analyzed the planktonic foraminifera of marls intercalated in the calcarenites, assigning a late Danian age to the Formation. Instead, the nannoplankton of the marls immediately underlying and overlying the unit are from the early Danian and the middle Selandian, respectively (Vera et al., 2004; Molina et al., 2006). These findings indicate that the Majalcorón and Olivares Formations likely share a similar, if not identical, age.

The most frequent internal sedimentary structures of the calcarenites are parallel laminations and hummocky-like structures (Vera et al., 2004, their Fig. 2). Based on the occurrence of the latter Vera et al. (2004) and Molina et al. (2006) concluded that the unit was deposited in a shallow ramp affected by storm waves. However, hummocky-like structures do not necessarily indicate shallow conditions, as they have also been documented in deep marine settings (e.g., Pomar et al., 2019). Besides, washed residues from marl samples collected immediately below and above the Majalcorón Formation are almost exclusively composed of planktonic foraminifera, a clear indication of deep marine conditions (Fig. S9C, D). Furthermore, the calcarenites of the Majalcorón Formation share similarities with those of the Olivares Formation, displaying internal parallel laminations topped by broad rounded ripples akin to those illustrated by Dumas et al. (2005; Fig. S9B, B′). Hence, it is logical to infer that the hummocky-like structures reported by Vera et al. (2004) and Molina et al. (2006) were shaped by deep marine currents. The influence of these currents likely accounts for the scarcity of marly intercalations within the calcarenites.

Descriptions of *Microcodium*-rich calcarenite deposits from other areas of the Subbetic Zone are rather general. For example, Martín-Algarra (1987, his Fig. 76) mentions accumulations approximately 100 m and 80 m thick near the Villanueva del Trabuco village and Sierra Prieta, both located to the north of Malaga (Fig. 1A). These accumulations predominantly comprise thick- and very thick-bedded calcarenites abundant in *Microcodium* remains, with lesser amounts of planktonic and benthic foraminifera, quartz, glauconite, and rock fragments. They are underlain and overlain by upper Maastrichtian and middle-upper Paleocene deposits, and are interpreted as originating from emerged carbonate massifs situated just south of the outcrops.

A comparable situation exists in the eastern Subbetic Zone. Smit (1979) reports several accumulations of Paleocene turbidites primarily comprising over 90 % of *Microcodium* remains between the villages of Vélez Rubio and Caravaca (Fig. 1A). In the so-named Melgoso section (location not specified), one of these accumulations is up to 130 m thick and consists of "practically amalgamated turbidites […] deposited within a single foraminiferal zone, the *Gl. uncinata* zone" (Smit, 1979, p. 45).

Information of the Capas Rojas Formation in the western part of the Subbetic Zone is notably scarce beyond the Alamedilla sector. This circumstance is somewhat surprising given the considerably broader outcrops of this unit compared to the *Microcodium*-rich calcarenites (Fig. 1C). As explained by Vera and Molina (1999), this scarcity primarily stems from the generally poor outcropping conditions of the unit, as its prevalent marly character is conducive to agricultural activities. Furthermore, most descriptions, such as those in maps produced at a 1:50.000 scale by the Spanish Geological Survey, overlook the delineation of the upper Cretaceous and Palaeogene segments of the unit. One of the few exceptions to this matter is provided by Martín-Algarra (1987), who documents a roughly 200 m thick Capas Rojas Formation of which only its uppermost 20–25 m are attributed to the Paleocene and early Eocene epochs.

Relevant geological data from the eastern Subbetic Zone is also scarce, but more precise. Within this area, the late Cretaceous-Eocene interval is represented by the Quipar-Jorquera Formation, a unit of similar lithology to that of the Capas Rojas Formation but of gray and brownish hues. In the Barranco del Gredero, near Caravaca (Fig. 1A), this formation is approximately 425 m thick, of which 225 m correspond to the Cenomanian-Maastrichtian, 120 m to the Paleocene, and 75 m to the Ypresian (Hillebrandt, 1974; Smit, 2004). According to these authors, the Paleocene succession in this section lacks detectable biostratigraphic hiatuses, accounting for its relatively substantial thickness. However, this circumstance appears to be an exception. For example, in the Aspe section, located about 100 km northeast of Caravaca (Fig. 1A), the Paleocene succession is only about 40 m thick and rests disconformably upon uppermost Maastrichtian marls (Hillebrandt, 1974, Fig. S9E, F). Notably, the early and middle Paleocene interval, during which *Microcodium*-rich calcarenites were accumulated elsewhere in the Subbetic Zone, is missing at the basal hiatus of this section.

5. Discussion

5.1. Olivares Formation

As stated above, the *Nereites* trace fossil association of the Olivares Formation calcarenites and the high planktonic/benthic foraminifera ratio in their intercalated marls (≈95 %) are clear evidence of deposition in a deep marine setting. Yet, the main components of the calcarenites of Members 1 and 2 are, by far, *Microcodium* remains (Figs. 3, S5), which also occur in significant proportions in Members 3 and 4 (Figs. 14C–F, S6A). These components must have been supplied from an emerged source area, since *Microcodium* is widely acknowledged to originate in terrestrial settings (Košir, 2004, 2015; Kabanov et al., 2008, and references therein). Most occurrences of late Cretaceous–Palaeogene *Microcodium* are documented in the European Mediterranean (or Tethys) region (Kabanov et al., 2008, their Fig. 2B). Calvet et al. (1991) and Pujalte et al. (2019) have indeed regarded it as a proxy for Mediterranean climate. Its origination in seasonally dry climates has also been suggested due to its frequent association with calcrete paleosols (Kabanov et al., 2008). Given that such climates are susceptible to sporadic heavy rainfall, it seems plausible that runoff following significant rains would transport *Microcodium* remains to the sea, potentially leading to the formation of thick calcarenites in the Olivares Formation and similar units during significant downpours.

The Ta and Tb intervals of medium and thick bedded calcarenites include, in addition to *Microcodium* aggregates, small amounts of resedimented ooids, miliolids and intraclasts with calpionellids (Figs. 3A, S5A–C). These components abound in Mesozoic carbonates outcropping in the NW flank of the Rio Fardes graben, specifically in the lower Jurassic (ooids and miliolids) and in the Berriasian (calpionellids; Comas, 1978; Comas et al., 1970; Fig. 4A, B). The derivation from these outcrops is further reinforced by palaeocurrents from flute marks (Fig. 4C). Both facts indicate that most, if not all the *Microcodium* remains came from emerged massifs of Mesozoic carbonates situated to the NW of the graben.

The Mesozoic outcrops reach today, after compression and inversion tectonics, a maximum height of 1447 m at Mencal Peak, about 750 m

above the Olivares Formation outcrops in the Fardes River valley (Fig. 4A, B), which provides a rough idea of the differential relief that might have existed originally between source and depositional areas. The fault-bounded character of the Mesozoic outcrops implies a rapid and abrupt transition from the emerged massifs into the deep-marine basin, which explains the conspicuous absence of resedimented shallow marine fauna in the Olivares Formation. The massive transfer of *Microcodium* to the deep sea was likely facilitated by that circumstance.

The great lateral extent of reference beds K, L and M (Fig. 7), coupled with their basal erosional surfaces and Ta/Tb intervals are clear proof of transportation by extensive turbidity currents. Likely this is also the case for most medium- and thick-bedded calcarenites having erosional bases and graded and/or parallel laminated intervals (Figs. 8 and 9). Additional transfer mechanisms may have been involved. For instance, the calcisiltites of Member 3 were accumulated in lower energy conditions, as evidenced by the absence of tractive structures and the preservation of internal bioturbations (Fig. 14C–E), and yet they also contain *Microcodium*. One of these mechanisms, favored by the rapid transition to deep waters, may have been density cascading, a process observed in the Bahama Banks (Wilson and Roberts, 1995), in the north-western Mediterranean (Puig et al., 2008) and in the Mauritius island (Slegel, 2022). In addition, transport of finer grains of *Microcodium* by wind during dry seasons cannot be excluded, although no conclusive proof has been found.

Regardless of their transfer mechanisms, once deposited on the seabed the calcarenites underwent reworking by other types of deep-sea currents, as indicated by their internal sedimentary structures and bedforms. However, determining the precise nature of some of these currents is difficult to ascertain. For instance, most medium- and thick-bedded calcarenites must have been emplaced by turbidity currents (as stated above), but the features of their upper Rwk divisions are at odds with what would be expected in a turbidite. In effect, cross-laminations of the Rwk intervals are bidirectional and never convoluted, the lower boundaries of cross-laminated sets are not flat but undulating, and individual cross-laminae may drape over these undulating boundaries (Fig. 8). Such cross-laminations differ notably from those of Bouma's Tc intervals, which are typically unidirectional and often convoluted, being instead akin to those created by oscillatory currents in shallow marine settings (e.g., de Raaf et al., 1977). Other features are reminiscent of tidal action, notably cross-laminated sets with flat or near flat lower boundaries but opposing palaeocurrent directions (Figs. 9, 13E). It is also tempting to attribute the rhythmic vertical alternations of thin and very-thin beds separated by clay drapes in Member 1 to tidal activity, as they are suggestive of principal and subordinate currents and slack waters, respectively. However, this attribution cannot be substantiated with palaeocurrents, as no internal laminations are observable in these beds (Fig. 11A–C).

Bedforms found at the upper surfaces of calcarenites also offer evidence of different types of currents. Thus, linguoid and sinuous asymmetrical ripples (Fig. S4C, D) and symmetrical ripples (Fig. S4E, F) are indicative of pure unidirectional and oscillatory currents, respectively. However, the ripples seen in profile in the Piornales section very likely resulted from the interaction of both types of currents (Fig. 12).

Considering all factors, it can be concluded that the majority of Olivares Formation calcarenites were carried into the deep sea by intermittent turbidity currents originating from the northwest margin of the graben. Once accumulated, the calcarenites were reworked by perhaps weaker but probably more persistent oscillatory and tidal currents that flowed along the graben. Given the nature and orientation of these bottom currents, they could be related to either internal waves or contour currents, or a combination of both (Huang et al., 2023).

The paucity of marls in the Olivares Formation, especially in Members 1 and 2 can also be explained in the context of persistent bottom currents. In effect, since the unit is intercalated within a marl-dominated succession, it seems unrealistic that during its deposition the influx of fine sediment would have diminished drastically. A more plausible alternative is that, besides reworking the calcarenites, the deep-sea currents acting within the graben also hindered the settling of finer particles. Interestingly, the proportion of marls in Member 1 increases gradually from the Olivares section to the Rio Gor section (Fig. 11). The former is closer to the fault-bounded NW margin of the graben, the latter farther afield. This fact entails that the farther from the marginal reliefs of the graben, the lesser was the intensity of the currents that hampered the deposition of marls.

In this context, the rhythmic alternation of thin marl-rich intervals and thick marl-poor calcarenite packages in Member 1 of the Olivares and Piornales sections can be attributed to periodic variations in the intensity of the currents, the intervals with weaker currents facilitating the deposition of marls (Fig. 10). In the Piornales section, the best exposed of the two, six of these alternations have been recognized (Fig. 10B). Interestingly, estimations of the duration of the P2 biozone, during which Member 1 was essentially developed, range between 400 and 700 kyr (Wade et al., 2011; Dinarès-Turell et al., 2014). It is therefore possible that the marl-rich/marl-poor alternations of Member 1 were linked to strengthening/weakening of bottom currents forced by Milankovitch eccentricity cycles, but more data are needed to confirm or reject this hypothesis.

5.2. The Capas Rojas Formation in the Alamedilla and Fardes-Gor sectors

The features of the late Maastrichtian–middle Danian and late Thanetian–Ypresian intervals of the Capas Rojas Formation are similar in the Alamedilla and Rio Gor sectors. In effect, these intervals are dominated in both cases by hemipelagic marls that, in coeval segments of the unit, exhibit the same colors, whether pink, red or gray (Figs. 2, 16). The PETM is also recorded in both sectors (Fig. 2). It should be mentioned, however, that the thickness of these intervals is greater at Rio Gor than at Alamedilla, and that turbidites are intercalated in the former section but almost absent in the latter. The K/Pg boundary interval is missing in Alamedilla and perhaps also in Rio Gor, but otherwise few biotratigraphically detectable hiatuses have been documented in the above mentioned intervals (Figs. 2A, S7A). Such evidence indicates that hemipelagic sedimentation was reasonably continuous in the whole study area during the late Maastrichtian–middle Danian and late Thanetian–Ypresian intervals.

In strong contrast, hemipelagic sedimentation in the Alamedilla sector was rather discontinuous during the late Danian–early Thanetian interval. In fact, this interval is entirely missing in two sections revisited in this study (Valencianos and Barranco, Fig. 16B, C) and almost absent in the Cejo 2 and Pedro Matínez sections studied by Pujalte et al. (2014b; Fig. S7A). In all cases, the strata above and below the boundary are clearly parallel, which confirms a disconformity relationship ("main disconformity" in Fig. 16).

The results of Martínez-Gallego (1977) in the Valencianos section are in line with this study, except that this author did find a 35–45 cm thick interval pertaining to the late Danian P2 biozone (Fig. S8C). Interestingly, the samplings for this study and that of Martínez-Gallego (1977) were carried out along different transects of the outcrop separated by about 30 m (P and MG in Fig. 16C), a proof that the temporal extent of the hiatus changes even over short distances. This possibility is further supported by the results in the two sections sampled in the Rambla Cejo (Rambla = dry creek), situated about 300 m from each other (Fig. 15): Cejo 1 contains P2, P3 and P4ab biozones, while in the Cejo 2 section only P2 is preserved (Figs. 16D, S7, S8A). However, it must be emphasized that the thicknesses of biozones P2, P3 and P4ab, when they are represented, are always very small. Thickness of P2, for example, ranges between 35 and 45 cm (Fig. S8). The duration of this biozone is estimated at 400–700 kyr (Wade et al., 2011; Dinarès-Turell et al., 2014), which would demand either an extremely reduced accumulation rate (between 0.5 and 1.1 mm/kyr) or, much more likely, that the biozone is riddled with diastems. Similar estimations can be made for the other two biozones.

The existence of these widespread hiatuses was implicit in the data of Martínez-Gallego (1977) and explicitly illustrated in those of Pujalte et al. (2014b; Fig. S7A). However, neither study provided an explanation of the origin and meaning of the hiatuses, likely because of the lack of the appropriate context. Here it is shown that the late Danian–early Thanetian interval, missing totally or partially at Alamedilla, is recorded at Rio Gor by two successive units, the upper Danian-lower Selandian Olivares Formation and the upper Selandian-lower Thanetian segment of the Capas Rojas Formation (Fig. 2B). The Olivares Formation provides convincing evidence of the action of persistent deep-sea currents in the area. Therefore, it is reasonable to assume that the Alamedilla hiatuses were also caused by similar currents, albeit perhaps weaker than those at Rio Gor. Indeed, widespread hiatuses and marked thickness changes in hemipelagic successions have been attributed to the action of weak bottom-current (Stow and Smillie, 2020, and references therein).

5.3. Palaeogeographic evolution

According to Vera and Molina (1999), the Upper Cretaceous—Eocene Capas Rojas Formation of the Subbetic Zone partly fossilized a faulted submarine palaeorelief resulting from several Mesozoic rifting phases. Their research highlights significant bathymetric differences of several hundred meters between uplifted and downfaulted blocks (their Fig. 5D–F), with the elevated blocks reaching depths of around 200 m. The findings presented in this paper align with this scenario, indicating that the Jurassic massifs along the Rio Fardes graben border correspond to uplifted blocks, while the graben itself and the Alamedilla sector represent downfaulted blocks. This study introduces new insight into successive phases within the late Maastrichtian–early Eocene interval, contributing to a more refined understanding of the palaeogeographic evolution of the Subbetic Zone during that period (Fig. 17).

During the Cretaceous and Palaeogene epochs, the Subbetic Zone was situated on the southern margin of the Iberian Plate, with the Tethys Ocean to the east, the proto-Atlantic Ocean to the west and the African Plate to the south, both plates being separated by a seaway. Martín-Chivelet et al. (2003) reported calcareous contourites in the upper Campanian to lower Maastrichtian succession near Caravaca (Subbetic Zone), and suggested their link with a westward-directed circumglobal surface current that flowed through this seaway, and/or a possible eastward-flowing subsurface current. It is also plausible, but difficult to prove (or disprove), that, similarly to today a deep thermohaline current also flowed through the seaway. However, such currents had minimal or no impact in the study area during the late Maastrichtian–middle Danian interval, as evidenced by the nearly analogous hemipelagic successions in both the Rio Gor and Alamedilla sectors (pre-archipelago phase in Fig. 17).

The mass-wasting accumulation situated 1–2 m below the Olivares Formation (Fig. S3) heralds the transition to the archipelago phase (Fig. 17). This accumulation was triggered by a short-lived tectonic event, which intensified previous bathymetric differences, ultimately culminating in the exposure of the highest sections of uplifted Mesozoic blocks. In the Fardes-Gor sector this event likely resulted from the reactivation of the faults bounding the graben. The simultaneous apparition of thick units of resedimented *Microcodium*-rich calcarenites throughout the Subbetic Zone suggests that the event was regional rather than local. The subaerially exposed parts of these blocks were colonized by *Microcodium*-producing plants, which were adapted to thrive in carbonate-rich substrates. Large amounts of *Microcodium* remains were delivered to the deep sea by turbidity currents and, possibly, also by density cascading, accumulating as calcarenites in the Rio Fardes graben and other depressed parts of the Subbetic Zone. However, away from the emerged massifs, hemipelagic sedimentation persisted in most parts of the Subbetic Zone, as in the Alamedilla sector (Fig. 1).

The emergence of the massifs brought about a notable transformation in the dynamics of sea currents within the study area, caused by a confluence of interacting factors. Firstly, the massifs effectively reduced the cross-sectional space of the seaway, increasing the velocity of the currents in accordance with the equation of continuity. Simultaneously, the more intricate bathymetric configuration and narrowed passages favored the formation of internal waves, which, upon colliding with sloping surfaces, gave rise to turbulence (Susanto et al., 2005; Pomar et al., 2012; St. Laurent et al., 2012). Furthermore, even in the absence of internal waves, sea mountains can independently generate turbulence, as highlighted by Voosen (2022). A logical inference is that turbulence would be greater closer to the mountains, which explains why the scarcity of marly interbeds is most pronounced in the Olivares section, which is the closest to the margin of the graben. The reworking of the Olivares Formation calcarenites and the presence of extensive hiatuses in the coeval hemipelagic deposits in the Alamedilla sector can both be attributed to the intensified submarine currents (Fig. 17). This underscores the significant impact of changing hydrodynamic conditions on sedimentological processes during the archipelago phase.

A relative sea level rise occurred during the deposition of the Olivares Formation, which caused a progressive submergence of the carbonate massifs and a reduction of the habitat of *Microcodium*-producing plants and the conclusion of the archipelago phase. The first part of this sea level rise is recorded by trace fossil associations, those in Member 2 indicating deeper conditions than those in Member 1 (Rodriguez-Tovar et al., 2020). The second part, within Members 3 and 4, is recorded by a decrease in the number of *Microcodium*-rich calcarenites and a simultaneous increase in planktonic foraminifera-rich and mixed-composition calcarenites.

During the post-archipelago phase, marked by the cessation of *Microcodium* influx into the Rio Fardes graben, hemipelagic sedimentation encroached on both the Rio Gor and Alamedilla sectors. Nevertheless, this phase can be further subdivided into two distinct subphases (Fig. 17).

Subphase 1, which spans the late Selandian–early Thanetian interval, is recorded in the Rio Gor sector by a ca. 75 m thick succession lacking discernible biostratigaphic hiatuses (Figs. 2B and 17). Conversely, in the Alamedilla sector, deposits of Subphase 1 are absent in the Valencianos and Barranco sections and irregularly represented in the Cejo 1 and Pedro Martínez sections (Fig. S7A). These variations likely stem from the persistence of an underwater relief during subphase 1 and, consequently, of deep-sea currents. These currents, although of lower intensity compared to those of the archipelago phase, were still strong enough to accumulate fine-grained sediments in the Rio Gor sector and selectively winnow them in the Alamedilla sector.

During subphase 2 (late Thanetian–early Eocene) a nearly uniform hemipelagic sedimentation encroached progressively on both the Rio Gor and Alamedilla sectors (Fig. 17). This fact suggests a gradual reduction in current intensity, likely associated to the attenuation of sea floor relief.

6. Conclusions

This paper presents a compelling case study of the impact of submarine topography on ancient deep-sea currents. The study was conducted in the central part of the Subbetic Zone of southern Spain, but the conclusions drawn can be extrapolated to the entire Zone based on information from geological literature. Throughout most of late Cretaceous to middle Eocene times this region was an open marine area with an irregular submarine landscape of tilted carbonate massifs. However, during the late Danian-early Selandian interval it evolved into an archipelago, as certain massifs emerged following a period of early-middle Danian tectonic unrest. Subsequently, due to erosion and subsidence, the emergent massifs were re-submerged, leading to the disappearance of the archipelago. These palaeogeographic changes were preserved in the stratigraphic record, thus offering a unique opportunity to inspect the characteristics of underwater currents across diverse seabed configurations.

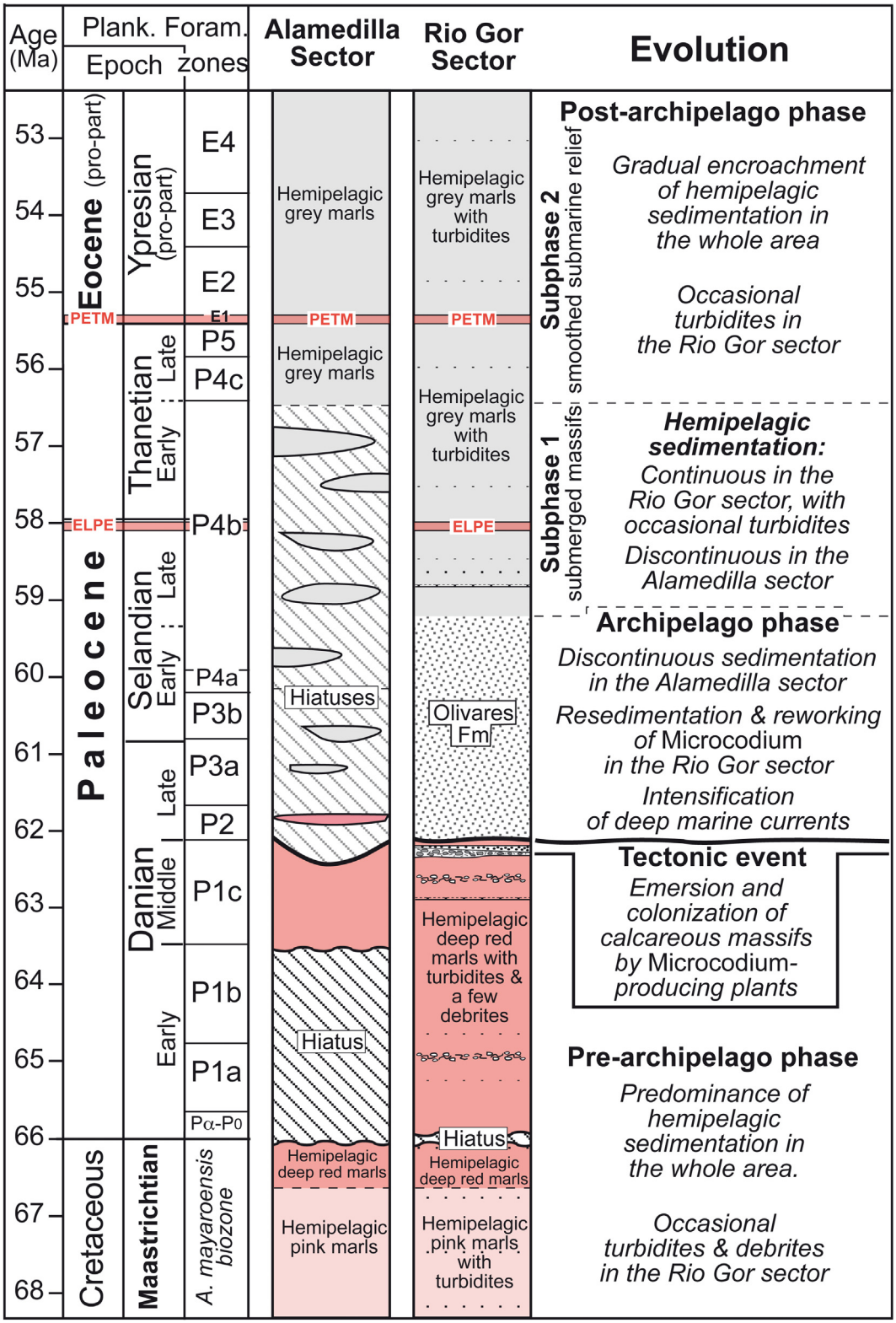

Fig. 17. Simplified sketch summarizing the evolutionary phases from the late Maastrichtian to the early Eocene in the Subbetic Zone, as deduced in this study. Explanation within the text.

During the late Cretaceous to middle Danian interval, prior to the formation of the archipelago, the slow accumulation of hemipelagic marls (Capas Rojas Formation) prevailed in the Subbetic Zone, best observed in the Alamedilla sector. Thicker successions of the Capas Rojas Formation, along with occasional turbidites, were deposited in topographic depressions of the region, such as the pre-existing Rio Fardes graben. It is noteworthy that during this interval, deep-sea currents must have been weak, as they exerted minimal to no influence on the dominant hemipelagic sedimentation.

During the archipelago phase (late Danian–Early Selandian), the emergent sections of the carbonate massifs became colonized by *Microcodium*-producing plants. Monocrystalline calcite grains of *Microcodium*, either isolated or as aggregates, were transferred to the deep sea by turbidity currents and, likely, also through density

cascading. This resulted in accumulations of calcarenites rich in these grains, in topographically depressed areas near the elevated massifs. Concurrently, hemipelagic sedimentation persisted in most other areas of the Subbetic Zone.

In contrast to the preceding phase, the newly emerged massifs within the archipelago compelled a notable increase in the velocity of deep marine currents, primarily by the combination of diminished cross-sectional space and turbulence induced by internal waves. Indicators of the heightened current activity, more prominent within the Olivares Formation, include: the partial or total reworking of *Microcodium*-rich calciturbidites by oscillatory currents; a variety of ripples and internal laminations shaped by both unidirectional, oscillatory and combined flows, some of them potentially originating from tidal forces; and last, but not least, the scarcity of marly deposits, particularly pronounced in the proximity of the emerged massifs, a clear indication of pervasive turbulence in their proximity. Although more subtly, the action of the intensified deep-sea currents is also imprinted in the coeval hemipelagic deposits of the Capas Rojas Formation of the Alamedilla sector, in this case by the presence of disconformities and hiatuses.

The subaerial parts of the massifs were progressively flooded as a result of a steady relative sea-level rise, marking the conclusion of the archipelago phase. Yet, for approximately 2 million years thereafter (late Selandian–early Thanetian), vestiges of submerged topography persisted, exerting a lasting influence on deep marine currents. The influence of these currents becomes evident in the numerous hiatuses present in the Alamedilla sector, some of which span the entirety of the interval. In strong contrast, the Rio Fardes Graben contains a comparatively thick and reasonably complete succession of marls interspersed with turbidites. It is conceivable that bottom currents winnowed the hemipelagic seabed at Alamedilla, but ponded and deposited sediments at Rio Gor.

The intensity of the currents gradually decreased from the late Thanetian onwards, in parallel with the attenuation of the sea floor relief. As a result, a near homogeneous hemipelagic sedimentation occurred throughout the Subbetic Zone, which persisted at least until the middle Eocene.

CRediT authorship contribution statement

Victoriano Pujalte: Writing – review & editing, Writing – original draft, Methodology, Investigation, Data curation, Conceptualization. **Aitor Payros:** Writing – review & editing, Project administration, Investigation, Funding acquisition, Formal analysis, Data curation. **Francisco J. Rodríguez-Tovar:** Writing – review & editing, Investigation, Data curation. **Xabier Orue-Etxebarria:** Writing – review & editing, Investigation, Data curation. **Naroa Martínez-Braceras:** Writing – review & editing, Investigation, Data curation.

Data availability

Data will be made available on request.

Declaration of competing interest

The authors declare the following financial interests/personal relationships which may be considered as potential competing interests: Aitor Payros reports that financial support was provided by Agencia Estatal de Investigación, Ministerio de Ciencia, Innovación y Universidades, Spain. Victoriano Pujalte reports that financial support was provided by Agencia Estatal de Investigación, Ministerio de Ciencia, Innovación y Universidades, Spain. Francisco J. Rodriguez-Tovar reports that financial support was provided by Agencia Estatal de Investigación, Ministerio de Ciencia, Innovación y Universidades, Spain. Naroa Martinez-Braceras reports that financial support was provided by Agencia Estatal de Investigación, Ministerio de Ciencia, Innovación y Universidades, Spain. If there are other authors, they declare that they have no known competing financial interests or personal relationships that could have appeared to influence the work reported in this paper.

Acknowledgments

We are indebted to two reviewers, Adrijan Košir from ZRC SAZU (Ljubljana) and an anonymous reviewer, as well as to editor Dr. Catherine Chagué, whose comments and suggestions significantly improved the original manuscript. The research by VP, AP, XO-E and NM-B was funded by project PID2019-105670GB-I00/AEI/10.13039/501100011033 (Agencia Estatal de Investigación, Ministerio de Ciencia, Innovación y Universidades, Spain) and by the Consolidated Research Group IT602-22 of the Basque Government. FR-T was funded by projects TED2021-131697B-C22 and PID2019-104625RB-100 (MCIN/AEI/10.13039/501100011033), Grant P18-RT-4074 (FEDER/Junta de Andalucía), and Research Group RNM-178 (Junta de Andalucía). NM-B is grateful for a Margarita Salas contract (MARSA22/05) of the Spanish Government with Next Generation funds from the European Union.

Appendix A. Supplementary data

Supplementary data to this article can be found online at https://doi.org/10.1016/j.sedgeo.2024.106648.

References

Alegret, L., Ortiz, S., 2009. Turnover at the sea floor during the Paleocene–Eocene Thermal Maximum: evidence from the Western Tethys. In: Crouch, E.M., Strong, C.P., Hollis, C.J. (Eds.), Climatic and Biotic Events of the Paleogene (CBEP 2009). CBEP International Conference, 12–15 January 2009, Wellington, New Zealand. GNS Science Miscellaneous Series18, pp. 9–13.

Alegret, L., Ortiz, S., Molina, E., 2009. Extinction and recovery of benthic foraminifera across the Paleocene–Eocene Thermal Maximum at the Alamedilla section (Southern Spain). Palaeogeography, Palaeoclimatology, Palaeoecology 279 (3), 186–200. https://doi.org/10.1016/j.palaeo.2009.05.009.

Alegret, L., Ortiz, S., Arenillas, I., Molina, E., 2010. What happens when the ocean is overheated? The foraminiferal response across the Paleocene-Eocene Thermal Maximum at the Alamedilla section (Spain). Geological Society of America Bulletin 122, 1616–1624. https://doi.org/10.1130/B30055.1.

Alonso, B., Ercilla, G., Casas, D., Stow, D.A., Rodríguez-Tovar, F.J., Dorador, J., Hernández-Molina, F.J., 2016. Contourite vs gravity-flow deposits of the Pleistocene Faro Drift (Gulf of Cadiz): sedimentological and mineralogical approaches. Marine Geology 377, 77–94. https://doi.org/10.1016/j.margeo.2015.12.016.

Alonso-Zarza, A.M., Sanz Montero, M.E., Calvo Sorando, J.P., Estévez López, P., 1998. Calcified root cells in Miocene pedogenic carbonates of the Madrid Basin: evidence for the origin of *Microcodium* b. Sedimentary Geology 16, 81–97. https://doi.org/10.1016/S0037-0738(97)00077-8.

Arenillas, I., Molina, E., 1996. Bioestratigrafía y evolución de las asociaciones de foraminíferos planctónicos del tránsito Paleoceno-Eoceno en Alamedilla (Cordilleras Béticas). Revista Española de Micropaleontología 28, 75–96 (in Spanish with English abstract).

Arz, J.A., 2000. Los foraminíferos planctónicos del Campaniense y Maastrichtiense: bioestratigrafia, Cronoestratigrafia y eventos paleoecológicos. (Ph.D. thesis), Prensas Universitarias de Zaragoza (419 pp.) (in Spanish with English abstract).

Aubry, M.-P., Ouda, K., Dupuis, C., Berggren, W.A., Van Couvering, J.A., 2007. The Global Standard Stratotype-section and Point (GSSP) for the base of the Eocene Series in the Dababiya section (Egypt). Episodes 30, 271–286. https://doi.org/10.18814/epiiugs/2007/v30i4/003.

Barnolas, A., Teixell, A., 1994. Platform sedimentation and collapse in a carbonate-dominated margin of a foreland basin (Jaca basin, Eocene, southern Pyrenees). Geology 22, 1107–1110. https://doi.org/10.1130/0091-7613(1994)022<1107:PSACIA>2.3.CO;2.

Bernaola, G., Baceta, J.I., Orue-Extebarria, X., Alegret, L., Martín-Rubio, M., Arostegui, J., Dinarès-Turell, J., 2007. Evidence of an abrupt environmental disruption during the mid-Paleocene biotic event (Zumaia section, western Pyrenees). Geological Society of America Bulletin 119, 785–795. https://doi.org/10.1130/B26132.1.

Brackenridge, R.E., Hernández-Molina, F.J., Stow, D.A.V., Llave, E., 2013. A Pliocene mixed contourite–turbidite system offshore the Algarve Margin, Gulf of Cadiz: seismic response, margin evolution and reservoir implications. Marine and Petroleum Geology 46, 36–50. https://doi.org/10.1016/j.marpetgeo.2013.05.015.

Calvet, F., Wright, V.P., Gimenez, J., 1991. *Microcodium*: descripción y origen: Implicaciones, paleogeográficas, paleoclimatológicas y paleogeomorfológicas. Actas Ier Congreso del Grupo Español del Terciario, Vic, Spain, pp. 50–55 (in Spanish).

de Castro, S., Hernández-Molina, F.J., Rodríguez-Tovar, F.J., Llave, E., Ng, Z.L., Nishida, N., Mena, A., 2020. Contourites and bottom current reworked sands: bed facies model and implications. Marine Geology 428, 106267. https://doi.org/10.1016/j.margeo.2020.106267.

Comas, M.C., 1978. Sobre la Geología de los Montes orientales. Sedimentación y evolución paleogeográfica desde el Jurásico al Mioceno inferior (zona Subbética, Andalucía). (Ph.D. thesis), University of Bilbao, Spain (323 pp.) (in Spanish).
Comas, M.C., García-Dueñas, V., González-Donoso, J.M., Rivas, P., 1970. Sobre el Jurásico del Mencal y su relación con otras series subbéticas de la transversal de Granada. Acta Geologica Hispánica 5, 77–81 (in Spanish with English abstract).
Comas, M.C., Delgado, F., Vera, J.A., 1973. Mapa Geológico de España 1:50.000, Hoja 993 (Benalúa de Guadix). IGME, Madrid (in Spanish).
Díaz de Neira, J.A., Enrile, A., López-Olmedo, F., 1988. Mapa Geológico de España 1:50.000, Hoja 970 (Huelma). Instituto Tecnológico y Geominero de España, Madrid (in Spanish).
Dinarès-Turell, J., Westerhold, T., Pujalte, V., Rölh, U., Kroon, D., 2014. Astronomical calibration of the Danian stage (Early Paleocene) revisited: settling chronologies of sedimentary records across the Atlantic and Pacific Oceans. Earth and Planetary Science Letters 405, 119–131. https://doi.org/10.1016/j.epsl.2014.08.027.
Dumas, S., Arnott, R.W.C., Southard, J.B., 2005. Experiments on oscillatory-flow and combined flow bed forms: implications for interpreting parts of the shallow-marine sedimentary record. Journal of Sedimentary Research 75 (3), 501–513. https://doi.org/10.2110/jsr.2005.039.
El Mamoune, B., 1996. Nannoplankton calcáreo del Paleógeno del Sur de España. (Ph.D. thesis), University of Granada, Spain (319 pp.) (in Spanish with English abstract).
Gonzalvo, C., Molina, E., 1998. Planktic foraminiferal biostratigraphy across the Lower-Middle Eocene transition in Betic Cordillera (Spain). Neues Jahrbuch Fur Geologie Und Palaontologie-Monatshefte 11. https://doi.org/10.1127/njgpm/1998/1998/671 671–603.
Hernández-Molina, F.J., de Castro, S., de Weger, W., Duarte, D., Fonnesu, M., Glazkova, T., Kirby, A., Llave, E., Ng, Z.N., Mantilla-Muñoz, O., Rodrigues, S., Rodríguez-Tovar, F.J., Thieblemont, A., Viana, A.R., Yin, S., 2022a. Chapter 9 - contourites and mixed depositional systems: a paradigm for deepwater sedimentary environments. In: Rotzien, Jon R., Yeilding, Cindy A., Sears, Richard A., Hernández-Molina, F. Javier, Catuneanu, Octavian (Eds.), Deepwater Sedimentary Systems. Elsevier, UK, pp. 301–360.
Hernández-Molina, F.J., Hüneke, H., Rodríguez-Tovar, F.J., Ng, Z.L., Llave, E., Mena, A., Gibb, A., Chiarella, D., Sammartino, S., de la Vara, A., 2022b. Eocene to middle Miocene contourite deposits in Cyprus: a record of Indian gateway evolution. Global and Planetary Change 219, 103983.
Hillebrandt, A., 1974. Bioestratigrafía del Paleogeno en el Sureste de España (Provincias de Murcia y Alicante). Cuadernos de Geología. Universidad de Granada 5, 135–153 (in Spanish).
Huang, L., Yang, J., Ma, Z., Liu, B., Ren, L., Liu, A.K., Chen, P., 2023. High-frequency obervations of oceanic internal waves from geostationary orbit satellites. Ocean-Land-Atmosphere Research 2, 0024. https://doi.org/10.34133/olar.0024.
Hüneke, H., Henrich, R., 2011. Pelagic sedimentation in modern and ancient oceans. In: Hüneke, H., Mulder, T. (Eds.), Deep-sea Sediments. Elsevier, Amsterdam, The Netherlands, pp. 215–351 https://doi.org/10.1016/B978-0-444-53000-4.00004-4.
Hüneke, H., Hernández-Molina, F.J., Rodríguez-Tovar, F.J., Llave, E., Chiarella, D., Mena, A., Stow, D.A.V., 2021. Diagnostic criteria using microfacies for calcareous contourites, turbidites and pelagites in the Eocene–Miocene slope succession, southern Cyprus. Sedimentology 68, 557–592. https://doi.org/10.1111/sed.12792.
Ito, M., 2002. Kuroshio current-influenced sandy contourites from the Plio-Pleistocene Kazusa forearc basin, Boso Peninsula. Japan. Geological Society, London, Memoirs 22 (1), 421–432. https://doi.org/10.1144/GSL.MEM.2002.022.01.29.
Jackson, C.R., 2004. An Atlas of Internal Solitary-like Waves and Their Properties. Global Ocean Associates, Rockville, MD (prepared for Office of Naval Research). [Online-31/01/2024] http://www.internalwaveatlas.com.
Kabanov, P., Anadón, P., Krumbein, W.E., 2008. *Microcodium*: an extensive review and a proposed non-rhizogenic biologically induced origin for its formation. Sedimentary Geology 205, 79–99. https://doi.org/10.1016/j.sedgeo.2008.02.003.
Klappa, C.F., 1978. Biolithogenesis of *Microcodium*: elucidation. Sedimentology 25, 489–522. https://doi.org/10.1111/j.1365-3091.1978.tb02077.x.
Košir, A., 2004. *Microcodium* revisited: root calcification products of terrestrial plants on carbonate-rich substrates. Journal of Sedimentary Research 74, 845–857. https://doi.org/10.1306/040404740845.
Košir, A., 2015. Ancient *Microcodium* and modern calcifed roots: spot the differences! Abstracts of 31st IAS Meeting of Sedimentology held in Krakow on 22nd–25th of June 2015. Polish Geological Society, Kraków, p. 281.
Linares, D., 1977. Estudio de los foraminiferos planctónicos del Cretácico superior de las Cordilleras Béticas (sector central). (Ph.D. thesis), University of Granada (410 pp.) (in Spanish).
Lu, G., Keller, G., Adatte, T., Ortiz, N., Molina, E., 1996. Long-term (10^5) or short-term (10^3) $\delta^{13}C$ excursion near the Palaeocene-Eocene transition: evidence from the Tethys. Terra Nova 8 (4), 347–355. https://doi.org/10.1111/j.1365-3121.1996.tb00567.x.
Lu, G., Adatte, T., Keller, G., Ortiz, N., 1998. Abrupt climatic, oceanographic and ecological changes near the Paleocene-Eocene transition in the deep Tethys basin: the Alamedilla section, southern Spain. Eclogae Geologicae Helvetiae 91, 293–306.
Martín-Algarra, A., 1987. Evolución geológica alpina del contacto entre las Zonas Internas y las Zonas Externas de la Cordillera Bética (sector central y occidental). (Ph.D. thesis), University of Granada (1271 pp.) (in Spanish).
Martín-Chivelet, J., Fregenal-Martínez, M., Chacón, B., 2003. Mid-depth calcareous contourites in the latest Cretaceous of Caravaca (Subbetic Zone, SE Spain). Origin and palaeohydrological significance. Sedimentary Geology 163, 131–146. https://doi.org/10.1016/S0037-0738(03)00176-3.
Martínez del Olmo, W., 2018. Episodios de deformación de la Cordillera Bética y su entorno próximo (España): problemas no resueltos. Revista de la Sociedad Geológica de España 31, 49–65 (in Spanish with English abstract).
Martínez-Gallego, J., 1977. Estudio micropaleontológico del Nummulítico de un sector comprendido entre Moreda-Piñar-Pedro Martínez (Zona Subbética). (Ph.D. thesis), University of Granada (241 pp.) (in Spanish).
Martínez-Gallego, J., Roca, A., 1973. Estudio del Danés de la cuenca nummulítica de Montefrío-Alcalá la Real. Correlación con el de Alamedilla (Zona Subbética). Cuadernos de Geología. Universidad de Granada 4, 93–97 (in Spanish).
Miguez-Salas, O., Rodríguez-Tovar, F.J., 2021. Trace fossil analysis of sandy clastic contouritic deposits in the late Miocene Rifian Corridor (Morocco): ichnotaxonomical and palaeoenvironmental insights. Journal of African Earth Sciences 174, 104054. https://doi.org/10.1016/j.jafrearsci.2020.104054.
Molina, J.M., Vera, J.A., Aguado, R., 2006. Reworked *Microcodium* calcarenites interbedded in pelagic sedimentary rocks (Paleocene, Subbetic, southern Spain): paleoenvironmental reconstruction. In: Alonso-Zarza, M.A., Tanner, L.H. (Eds.), Paleoenvironmental Record and Applications of Calcretes and Palustrine Carbonates. Geological Society of America Special Papers416, pp. 189–202. https://doi.org/10.1130/2006.2416(12).
Molina, J.M., Reolid, M., Mattioli, E., 2007. Thin-shelled bivalve ("filament") buildup of the Aalenian-lowest Bajocian in the Subbetic (South Iberian Paleomargin). Geogaceta 61, 31–34 (in Spanish with English abstract).
Monechi, S., Angori, E., Von Salis, K., 2000. Calcareous nannofossil turnover around the Paleocene/Eocene transition at Alamedilla (southern Spain). Bulletin de la Société géologique de France 171, 477–489. https://doi.org/10.2113/171.4.477.
Payros, A., Pujalte, V., Orue-Etxebarria, X., 1999. The South Pyrenean Eocene carbonate megabreccias revisited: new interpretation based on evidence from the Pamplona Basin. Sedimentary Geology 125, 165–194. https://doi.org/10.1016/S0037-0738(99)00004-4.
Pomar, L., Morsilli, M., Hallock, P., Bádenas, B., 2012. Internal waves, an under-explored source of turbulence events in the sedimentary record. Earth Science Reviews 111, 56–81. https://doi.org/10.1016/j.earscirev.2011.12.005.
Pomar, L., Molina, J.M., Ruiz-Ortiz, P.A., Vera, J.A., 2019. Storms in the deep: tempestite- and beach-like deposits in pelagic sequences (Jurassic, Subbetic, South of Spain). Marine and Petroleum Geology 107, 365–381. https://doi.org/10.1016/j.marpetgeo.2019.05.029.
Puig, P., Palanques, A., Orange, D.L., Lastras, G., Canals, M., 2008. Dense shelf water cascading and furrows formation in the Cap de Creus Canyon, northwestern Mediterranean Sea. Continental Shelf Research 28, 2017–2030. https://doi.org/10.1016/j.csr.2008.05.002.
Pujalte, V., Orue-Etxebarria, X., Apellaniz, E., Caballero, F., Robles, S., 2012. Río Gor, comarca de Guadix, provincia de Granada: una nueva sección de referencia del Paleógeno inferior Subbético. Geogaceta 52, 53–56 (in Spanish with English abstract).
Pujalte, V., Orue-Etxebarria, X., Apellaniz, E., Caballero, F., Monechi, S., Ortiz, S., Schmitz, B., 2014a. A prospective Early Late Paleocene event (ELPE) from the expanded Río Gor hemipelagic section (Betic Cordillera, southern Spain): foraminifera, nannofossil and isotopic data. Rendiconti Online della Società Geologica Italiana 31, 181–182. https://doi.org/10.3301/ROL.2014.110.
Pujalte, V., Orue-Etxebarria, X., Apellaniz, E., Caballero, F., 2014b. El Paleógeno inferior de los Montes Orientales, provincia de Granada, Zona Subbética: revisión y nuevos datos. Revista de la Sociedad Geológica de España 27, 137–149 (in Spanish with English abstract).
Pujalte, V., Apellaniz, E., Caballero, F., Monechi, S., Ortiz, S., Orue-Etxebarria, X., Rodríguez-Tovar, F.J., Schmitz, B., 2017. Integrative stratigraphy and climatic events of a new lower Paleogene reference section from the Betic Cordillera: Río Gor, Granada province, SE Spain. Spanish Journal of Palaeontology 32, 185–206. https://doi.org/10.7203/sjp.32.1.17039.
Pujalte, V., Monechi, S., Ortiz, S., Orue-Etxebarria, X., Rodriguez-Tovar, F., Schmitz, B., 2019. *Microcodium*-rich turbidites in hemipelagic sediments during the Paleocene–Eocene Thermal Maximum: evidence for extreme precipitation events in a Mediterranean climate (Río Gor section, southern Spain). Global and Planetary Change 178, 153–167. https://doi.org/10.1016/j.gloplacha.2019.04.018.
de Raaf, J.F.M., Boersma, J.R., Van Gelder, S., 1977. Wave-generated structures and sequences from a shallow marine succession, Lower Carboniferous, County Cork, Ireland. Sedimentology 24 (4), 451–483. https://doi.org/10.1111/j.1365-3091.1977.tb00134.x.
Rebesco, M., Mosher, D., Piper, D.J.W., 2017. Advancements in Understanding Deep-Sea Clastic Sedimentation Processes: a preface. Marine Geology 393, 1–3. https://doi.org/10.1016/j.margeo.2017.10.007.
Rodríguez-Tovar, F.J., Hernández-Molina, F.J., 2018. Ichnological analysis of contourites: past, present and future. Earth Science Reviews 182, 28–41. https://doi.org/10.1016/j.earscirev.2018.05.008.
Rodríguez-Tovar, F.J., Hernández-Molina, F.J., Hünekec, H., Chiarella, D., Llave, E., Mena, A., Miguez-Salasa, O., Dorador, J., de Castro, S., Stow, D.A.V., 2019. Key evidence for distal turbiditic- and bottom-current interactions from tubular turbidite infills. Palaeogeography, Palaeoclimatology, Palaeoecology 533, 109233. https://doi.org/10.1016/j.palaeo.2019.109233.
Rodriguez-Tovar, F.J., Pujalte, V., Payros, A., 2020. Danian-lower Selandian *Microcodium*-rich calcarenites of the Subbetic Zone (SE Spain): record of *Nereites* ichnofacies in a deep-sea, base-of-slope system. Sedimentary Geology 406, 105723. https://doi.org/10.1016/j.sedgeo.2020.105723.
Rodríguez-Tovar, F.J., Miguez-Salas, O., Dorador, J., 2022. Deepwater ichnology: new observations on contourites. In: Rotzien, J.R., Yeilding, Cindy A., Sears, Richard A., Hernández-Molina, F.J., Catuneanu, O. (Eds.), Deepwater Sedimentary Systems. Elsevier, UK, pp. 533–554 https://doi.org/10.1016/B978-0-323-91918-0.00022-0.
Santo, D.S.U., Mitnik, L.D., Zheng, Q., 2005. Ocean internal waves observed in the Lombok Strait. Oceanography 18 (4), 81–89. https://doi.org/10.5670/oceanog.2005.08.
Sanz de Galdeano, C., 2019. Paleogeographic reconstruction of the Betic-Rif Internal Zone: an attempt. Revista de la Sociedad Geológica de España 32 (2), 107–128.
Schmitz, B., Pujalte, V., Molina, E., Monechi, S., Orue-Etxebarria, X., Speijer, R.P., Alegret, L., Apellaniz, E., Arenillas, I., Aubry, M.P., Baceta, J.I., Berggren, W.A., Bernaola, G., Caballero, F., Clemmensen, A., Dinarès-Turell, J., Dupuis, C., Heilman-Clausen, C., Hilario Orus, A., Knox, R., Martín-Rubio, M., Ortiz, S., Payros, A., Petrizzo, M.R., von Salis, K., Sprong, J., Steurbaut, E., Thomsen, E., 2011. The global stratotype section and points for the

bases of the Selandian (Middle Paleocene) and Thanetian (Upper Paleocene) stages at Zumaia, Spain. Episodes 34, 220–243. https://doi.org/10.18814/epiiugs/2011/v34i4/002.

Slegel, E., 2022. How an "underwater waterfall" came to exist on Mauritius. Big Think, Starts with a Bang, February 24, 2022 (last accessed 09/04/2024) https://bigthink.com/starts-with-a-bang/underwater-waterfall-mauritius/.

Smit, J., 1979. *Microcodium*, its earliest occurrence and other considerations. Revue de Micropaleontologie 22, 44–50.

Smit, J., 2004. The section of the Barranco del Gredero (Caravaca, SE Spain): a crucial section for the Cretaceous/Tertiary boundary impact extinction hypothesis. Journal of Iberian Geology 31, 179–191.

St. Laurent, L., Alford, M.H., Paluszkiewicz, T., 2012. An introduction to the special issue on internal waves. Oceanography 25, 15–19. https://doi.org/10.5670/oceanog.2012.37.

Stow, D., Smillie, Z., 2020. Distinguishing between deep-water sediment facies: turbidites, contourites and hemipelagites. Geosciences 10 (2), 68. https://doi.org/10.3390/geosciences10020068.

Susanto, R.D., Mitnik, L.D., Zheng, Q., 2005. Ocean internal waves observed in the Lombok Strait. Oceanography 18, 80–87. https://doi.org/10.5670/oceanog.2005.08.

Tucker, M., 1982. The Field Description of Sedimentary Rocks. Geological Society of London Handbook. Open University Press, Milton Keynes, UK and John Wiley & Sons, New York (112 pp.).

Vera, J.A., 2000. El Terciario de la Cordillera Bética: estado actual de conocimientos. Revista de la Sociedad Geológica de España 13, 345–373 (in Spanish with English abstract).

Vera, J.A., 2004. Cordillera Bética y Baleares. In: Vera, J.A. (Ed.), Geología de España. Sociedad Geológica de España (SGE) and Instituto Geológico y Minero de España (IGME), Madrid, pp. 347–464 (in Spanish).

Vera, J.A., Molina, J.M., 1999. La Formación Capas Rojas: Caracterización y Génesis. Estudios Geológicos 55, 45–66 (in Spanish with English abstract) https://doi.org/10.3989/egeol.99551-2181.

Vera, J.A., García-Hernández, M., López-Garrido, A.C., Comas, M.C., Ruiz-Ortíz, P.A., Martín-Algarra, A., 1982. El Cretácico de la Cordillera Bética. In: García, A. (Ed.), El Cretácico de España. Editorial Complutense, Madrid, pp. 515–632 (in Spanish).

Vera, J.A., Molina, J.M., Aguado, R., 2004. Calcarenitas de *Microcodium* (Formación Majalcorón, Paleoceno, Subbético): descripción, bioestratigrafía y significado en el Terciario de la Cordillera. Boletín Geológico y Minero 115, 453–468 (in Spanish with English abstract).

Voosen, P., 2022. Undersea mountains stir up currents critical to Earth's climate. Science 375, 1324–1325. https://doi.org/10.1126/science.abq1934.

Wade, B.S., Pearson, P.N., Berggren, W.A., Pälike, H., 2011. Review and revision of Cenozoic tropical planktonic foraminiferal biostratigraphy and calibration to the geomagnetic polarity and astronomical time scale. Earth Science Reviews 104, 111–142. https://doi.org/10.1016/j.earscirev.2010.09.003.

Wilson, P.A., Roberts, H.H., 1995. Density cascading: off-shelf sediment transport, evidence and implications, Bahama Banks. Journal of Sedimentary Research 65, 45–56. https://doi.org/10.1306/D426801D-2B26-11D7-8648000102C1865D.